

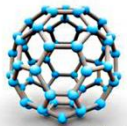


Dublin City University
School of Electronic Engineering

Copper Halide Semiconductors for Room Temperature Quantum Applications – A Materials Perspective

R.K. Vijayaraghavan, S. Daniels and P. McNally

School of Electronic Engineering, Dublin City University



APT

Advanced Processing Technology Research Centre



Nanomaterials
Processing Laboratory | **NPL**



NCPST National Centre
for Plasma Science
& Technology

Acknowledgements

- DCU: Aidan Cowley, Barry Foy, Francis Olabanji Lucas, Lisa O'Reilly, Prof. Enda McGlynn, Prof. Martin Henry.
- TCD: Anirban Mitra, Daniel Danieluk, Prof. Louise Bradley (TCD).

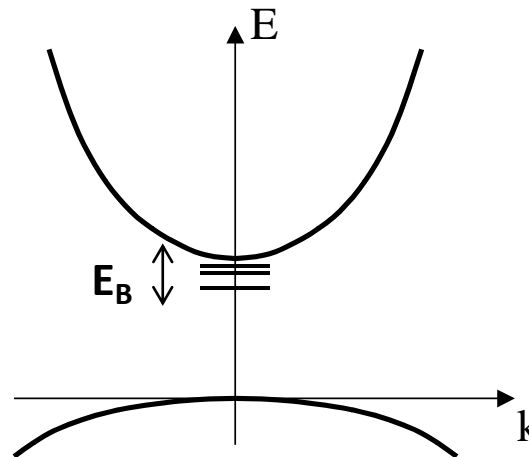
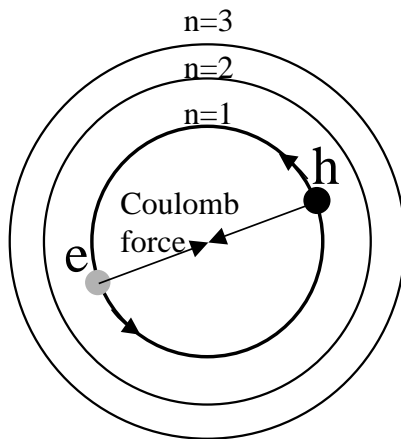
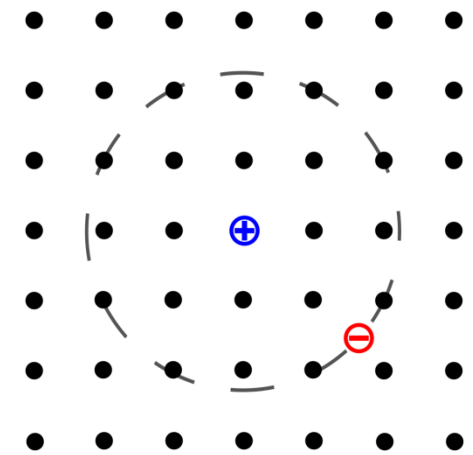


New Quantum Technologies

- Based on control and manipulation of quantum entities:
 - individual photons,
 - photons mixed with other physical particles, e.g. light-matter coupling,
 - excitonic, biexcitonic and polaritonic systems.
- Light-matter coupling can be implemented in the long wavelength red and infrared regions of the spectrum.
- “Spectral bottleneck” in the Blue/UV spectral region...350-450 nm.
- Precludes the fabrication of
 - useful Blue/UV ultra-low power (e.g. polaritonic) light emitting and laser diode sources,
 - the generation of room temperature quantum entanglement systems in the Blue/UV spectrum.

Quantum Quasiparticles

- Exciton (Wannier):
- Bound electron-hole pair
- Coulomb attraction



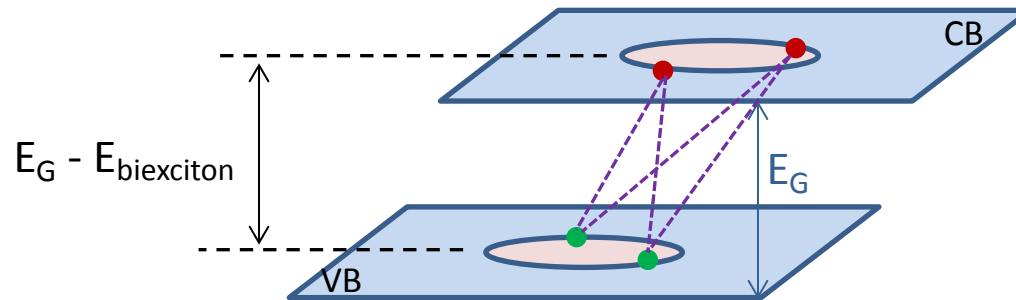
$$E_b = -\frac{m_r^* q^4}{2h^2 \epsilon^2} \frac{1}{n^2}$$

$$\frac{1}{m_r^*} = \frac{1}{m_e^*} + \frac{1}{m_h^*}$$

- Hydrogen-like bound states
- Binding energy $E_B \approx 10\text{meV}$
- Bohr Radius (a_B) $\approx 100\text{\AA}$
- Composite bosons

Quantum Quasiparticles

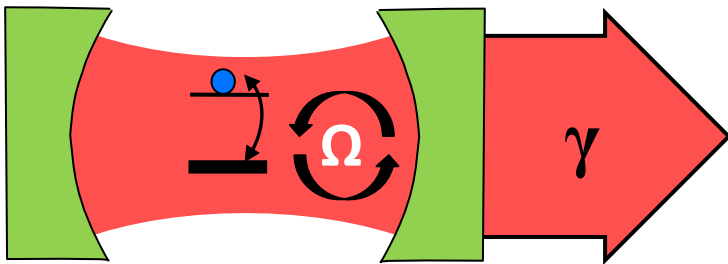
- **Biexcitons:**
- Exciton molecules



- Biexciton Binding Energies:
 - Typically $E_{\text{biexciton}} = 1-5 \text{ meV}$...very small
- Also composite bosons.

Quantum Quasiparticles

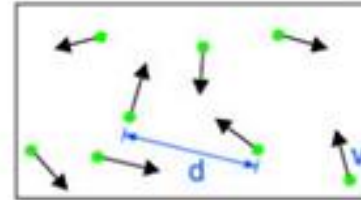
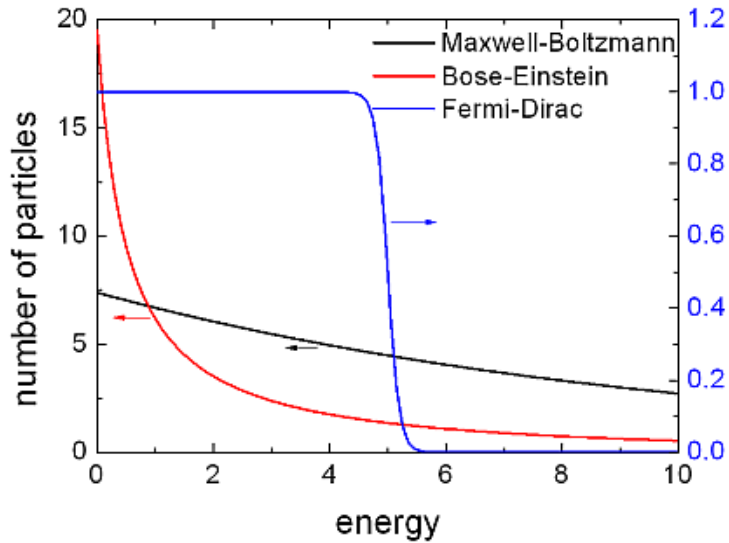
- Polaritons:
- Light-Matter Coupling \Rightarrow Microcavity
- Photons and Excitons couple
- Polariton-excitons \Leftrightarrow “Polaritons”



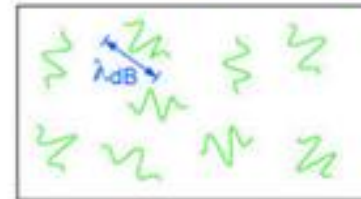
Ω = coupling strength between optical transition of the material and the resonance photon mode

γ = loss channel

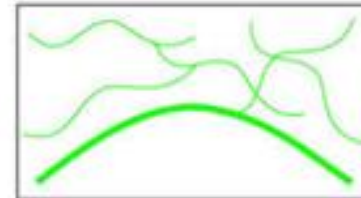
Bose-Einstein Statistics Prevail



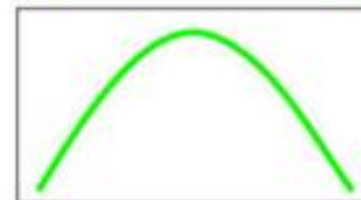
High Temperature T:
 thermal velocity v
 density d^{-3}
 "Billiard balls"



Low Temperature T:
 De Broglie wavelength
 $\lambda_{dB} = h/mv \propto T^{-1/2}$
 "Wave packets"



T = T_{crit}:
Bose-Einstein Condensation
 $\lambda_{dB} = d$
 "Matter wave overlap"



T = 0:
Pure Bose condensate
 "Giant matter wave"

The probability that a particle will have energy E

Describing integer spin bosons, this distribution allows an unlimited number of particles to condense into a single level.

$$f(E) = \frac{1}{Ae^{E/kT} - 1}$$

Bose-Einstein

For photons, $A=1$, so the occupation of very low energy states can increase without limit.

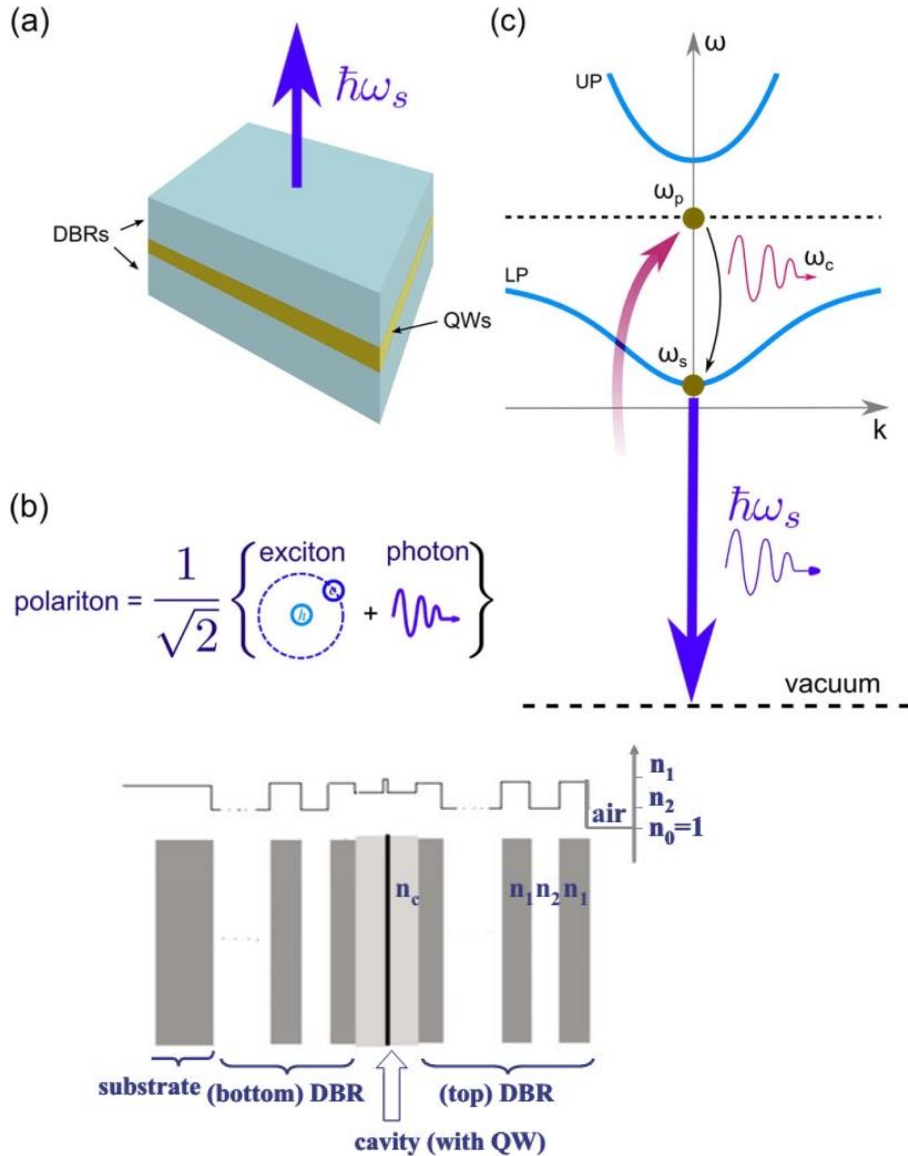
The quantum difference which arises from the fact that the particles are indistinguishable.

The exponential dependence upon energy and temperature. See the classical Boltzmann distribution for more description.

Sources:

hyperphysics.phy-astr.gsu.edu
 www.uni-muenster.de
 imagebank.osa.org

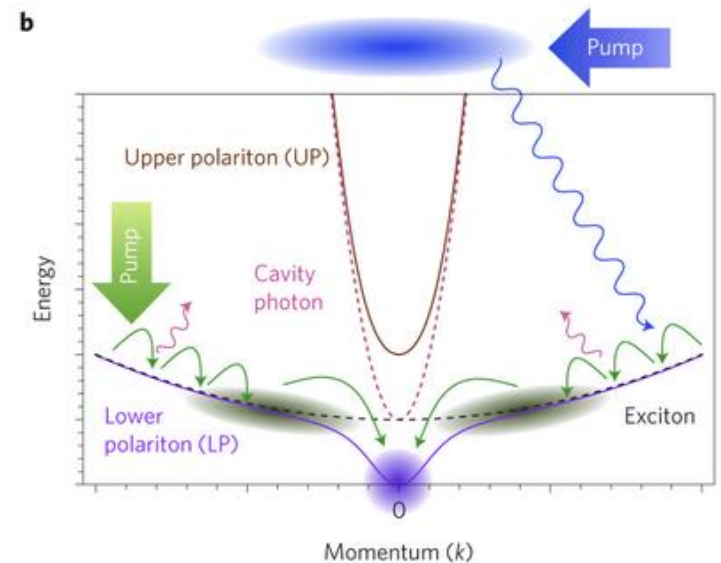
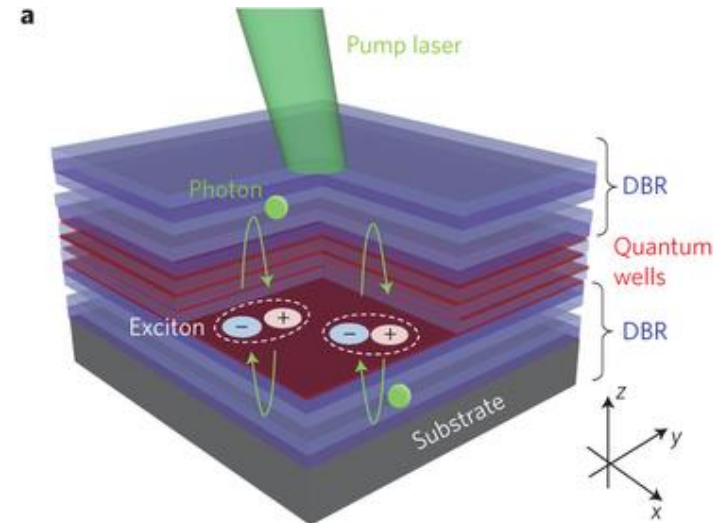
Polariton Lasing



Sources: M. Glazov, SPIE Newsroom, DOI: 10.1117/2.1201212.004623 & H Deng *et al.*, Rev. Mod. Phys. **82** (2010) 1489-1537.

Polariton Lasing

- (a) Polaritons are excited by a pump laser.
- (b) Strong coupling between the cavity photon and exciton dispersions split the dispersions near $k = 0 \Rightarrow$ creates a lower polariton (LP) and an upper polariton (UP) dispersions. Pump laser excites high energy excitons which cool via phonon emission towards the bottleneck region (black cloud). Excitons then scatter into the condensate via stimulated cooling.

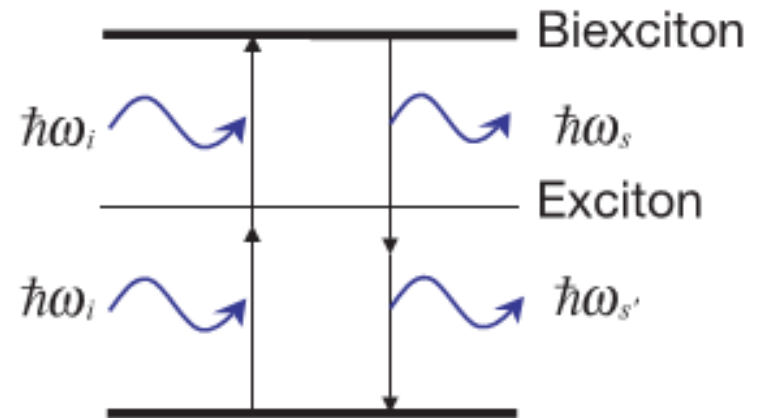


Polaritonic Light Emitters

- Polaritons behave like electrons/holes with an effective mass $\approx 1/10,000$ that of an electron!
- Different lasing mechanism possible \Rightarrow “polaritonic lasing”.
- Lasing threshold current densities 2-3 orders of magnitude lower than for conventional laser diodes (LDs).
- Conventional LD: $J_{th} = 10,000 \text{ Acm}^{-2}$
- Polaritonic LD: $J_{th} = 100 \text{ Acm}^{-2}$
- Ultra efficient; ultra low power light emission possible.

UV Entangled Photons

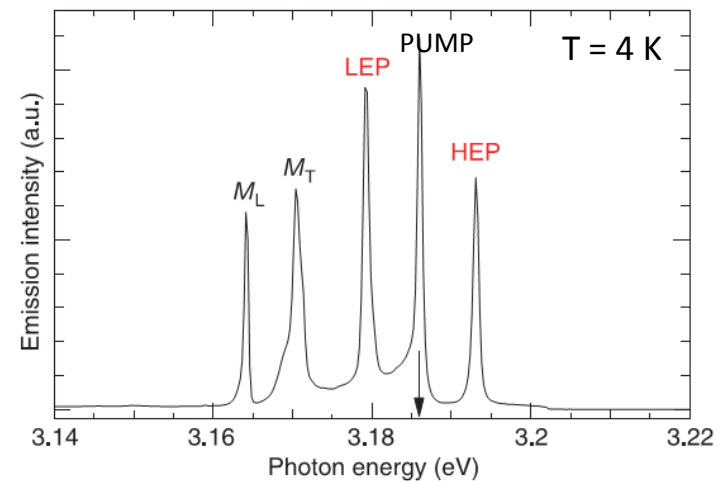
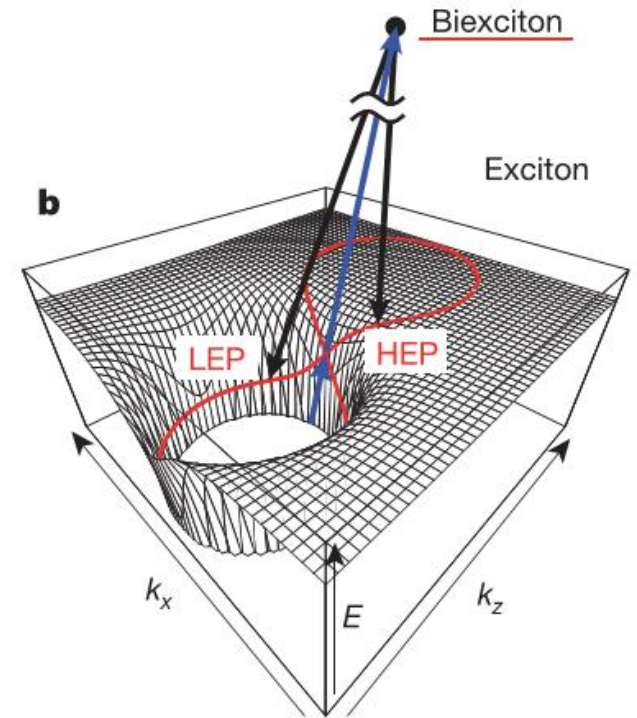
- Resonant Hyper-Parametric Scattering (RHPS)
- Generation of two entangled photons via electronically resonant third order nonlinear optical process.
- Copper halides - CuCl or CuBr - are ideal materials
- RHPS resonant to biexcitonic state.
- Two pump photons (frequency ω_i) resonantly create a biexciton.
- Biexcitonic state (Γ_1) has zero angular momentum, i.e. $J=0$.
- Scattered ENTANGLED (daughter) photons ($\omega_s, \omega_{s'}$)
- Emerge from the $J=0$ process.



Source: K Edamatsu *et al.*,
Nature **431** (2004) 167.

UV Entangled Photons

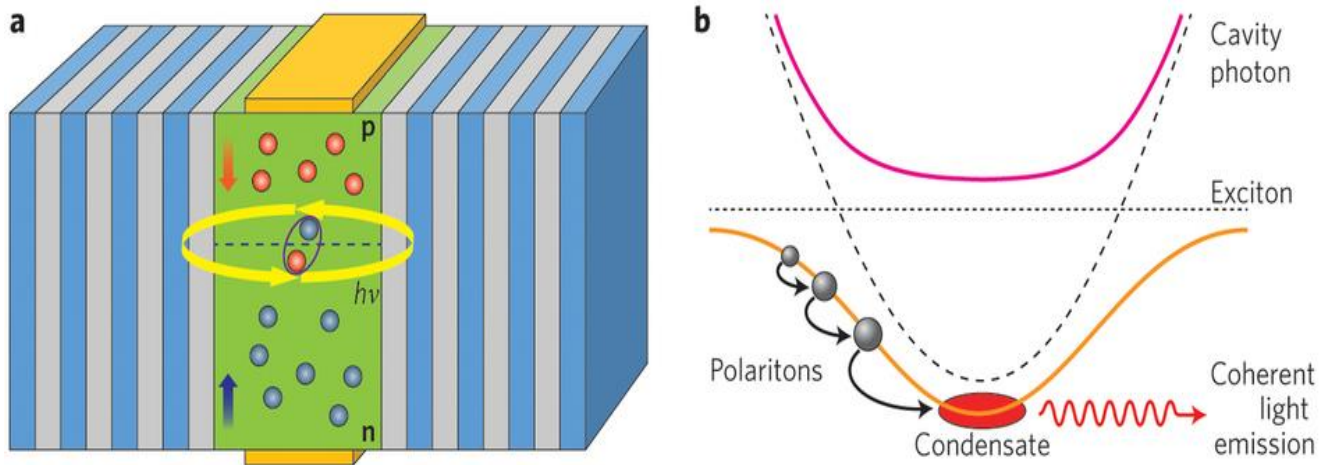
- Actual RHPS emission process \Rightarrow phase-matching condition involving polaritons.
- Biexciton coherently decays into two polaritons (sum of photon energies and momenta conserved).
- Lower energy polariton (LEP) and higher energy polariton (HEP).
- Polarisation entangled photons confirmed at 4 K by Edamatsu *et al.* (2004).



Source: K Edamatsu *et al.*,
Nature **431** (2004) 167.

BUT...

- **Optical pumping was used**
- **ELECTRICAL PUMPING preferred for field operation.**
- P. Bhattacharya *et al.* (2014) : Demonstrated room temperature electrically pumped GaN polaritonic LD.
- Current injection is orthogonal to the optical feedback direction of the resonator.
- $J_{th} = 169 \text{ Acm}^{-2}$. $\lambda \approx 365 \text{ nm}$.



Can we achieve superior operation?...

- Copper halide (CuHa) semiconductors possess much higher excitonic binding energies.
- The higher this energy the more likely is stable and continuous room temperature operation*.
- Biexcitonic binding energies are very high.
- More likely it is that the CuHa material can exhibit quantum entanglement effects, which are essential components of photonic quantum information processing and communication (QIPC) technologies.

Material	Excitonic Binding Energies	Biexcitonic Binding Energies	Material	Excitonic Binding Energies	Biexcitonic Binding Energies
γ -CuCl	190 meV**	34 meV	GaN	27 meV	20 meV &&
γ -CuBr	108 meV **	20 meV	ZnO	60 meV	15 meV &&
γ -CuI	62 meV	6 meV	GaAs	4.2 meV	1 meV

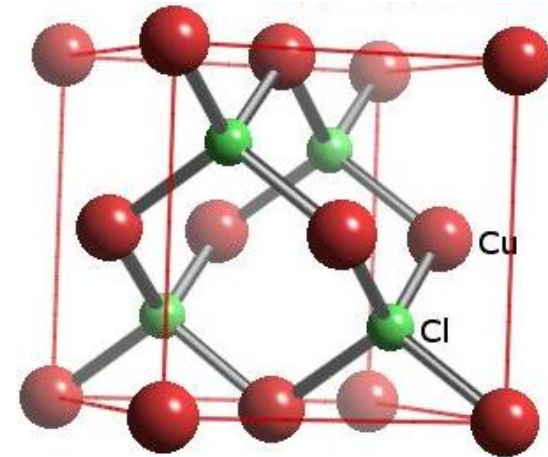
** Excitonic structure comprises of a number of closely spaced excitons e.g. $Z_{1,2}$ and Z_3 .

&& Typically achieved using quantum confinement e.g. multiple quantum wells (MQWs); CuHa data quoted is for bulk material but CuHa MQWs will see up to 5x enhancements [D. Ahn et al., Appl. Phys. Lett. 102, 121114 (2013)]

§ Source: "Semiconductors: Data Handbook", O. Madelung, (Springer-Verlag, Berlin, Germany (2004)).

The Copper Halides

- γ -CuCl; γ -CuBr: I-VII, cubic, zincblende semiconductor.
- Direct, wide bandgap.



Material	Room Temp. Bandgap (ev)	Exciton Binding Energy (meV)	Lattice Constant (nm)	Melting Point (Celsius)
Si	1.12	-	0.538	1414°
ZnO	3.37	60	0.324 (wurtzite)	1974°
GaN	5.43	23	0.438	2520°
CuCl	3.365	190	0.541	430°
CuBr	3.1	108	0.568	504°

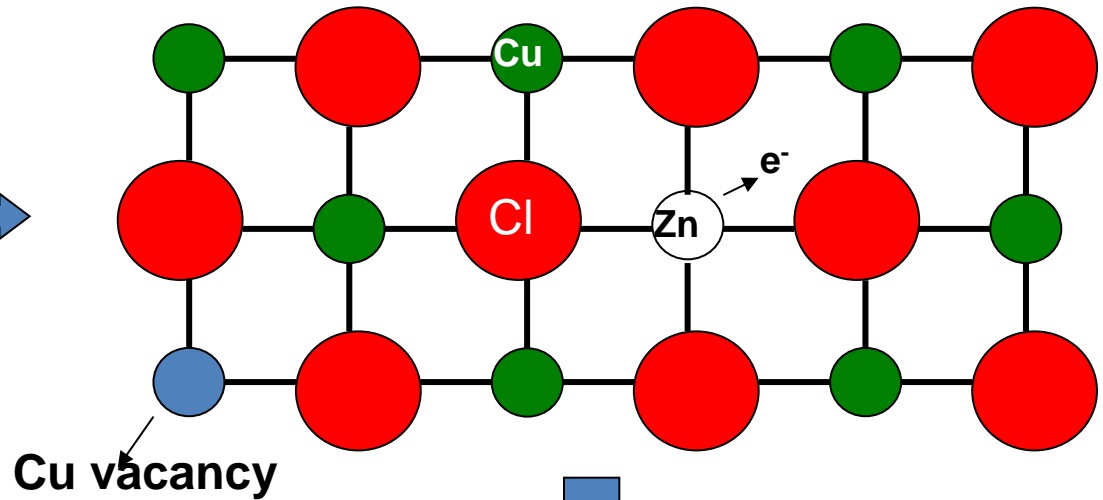
Requirements for CuHa polaritonic/biexcitonic electrically pumped device operation

- High quality doped active CuHa nanolayers:
 - n-CuCl; p-CuCl
 - n-CuBr; p-CuBr.
- Electrical contacts to CuHa layers.
- Microcavity confinement for polaritons.
- Encapsulation to maintain device operation.
- Significant recent advances meeting each of these requirements.

n-type CuI nanolayers: Zn doping

Zn Dopant: A group II element with almost similar ionic radii to Cu (≈ 60 pm)

Substitutional Zn in the Copper site \rightarrow



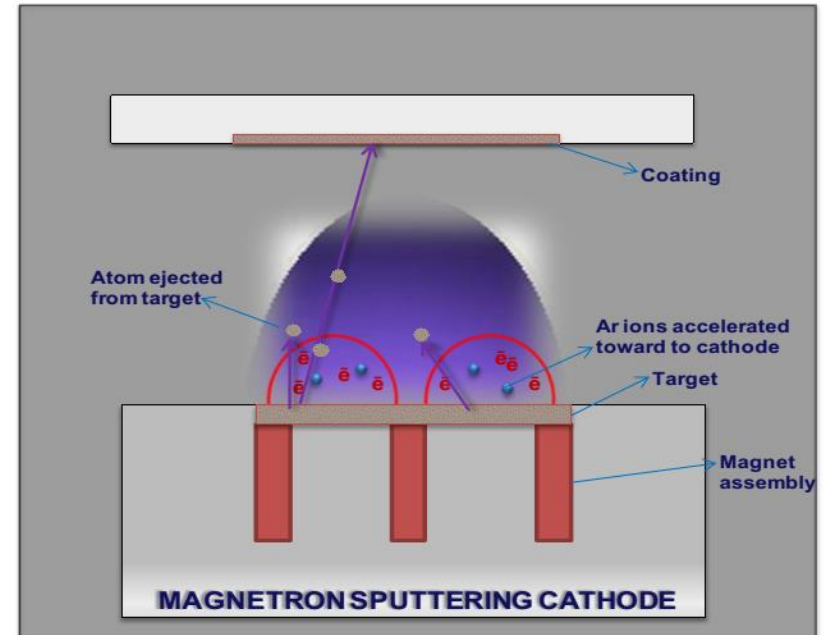
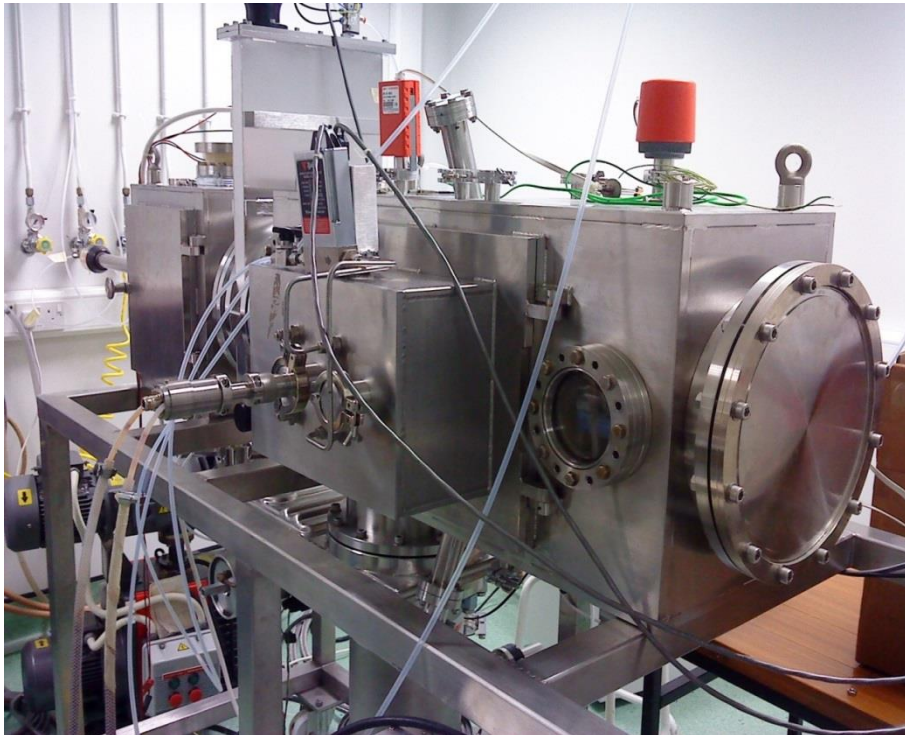
N-type CuI

Zn is an excellent donor for CuCl or CuBr.

Deposition method

Pulsed dc magnetron sputtering of a CuCl:Zn target at room temperature.

- Working pressure $\approx 5.5 \times 10^{-3}$ mbar
- Power density ≈ 1.75 W/cm²
- Pulse duty cycle $\approx 40\%$

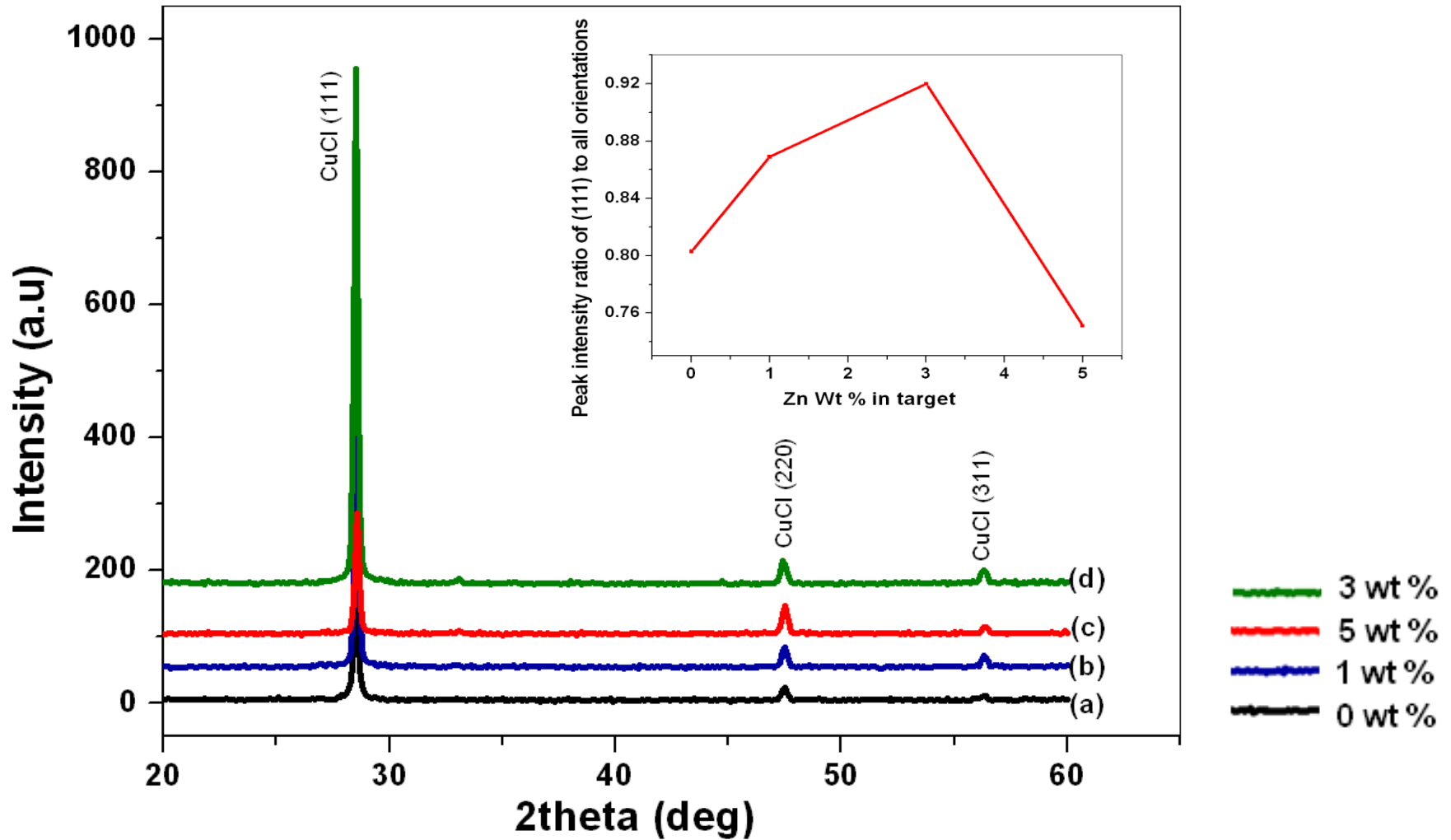


Advantages

- High deposition rate
- Manufacturability
- Good quality films

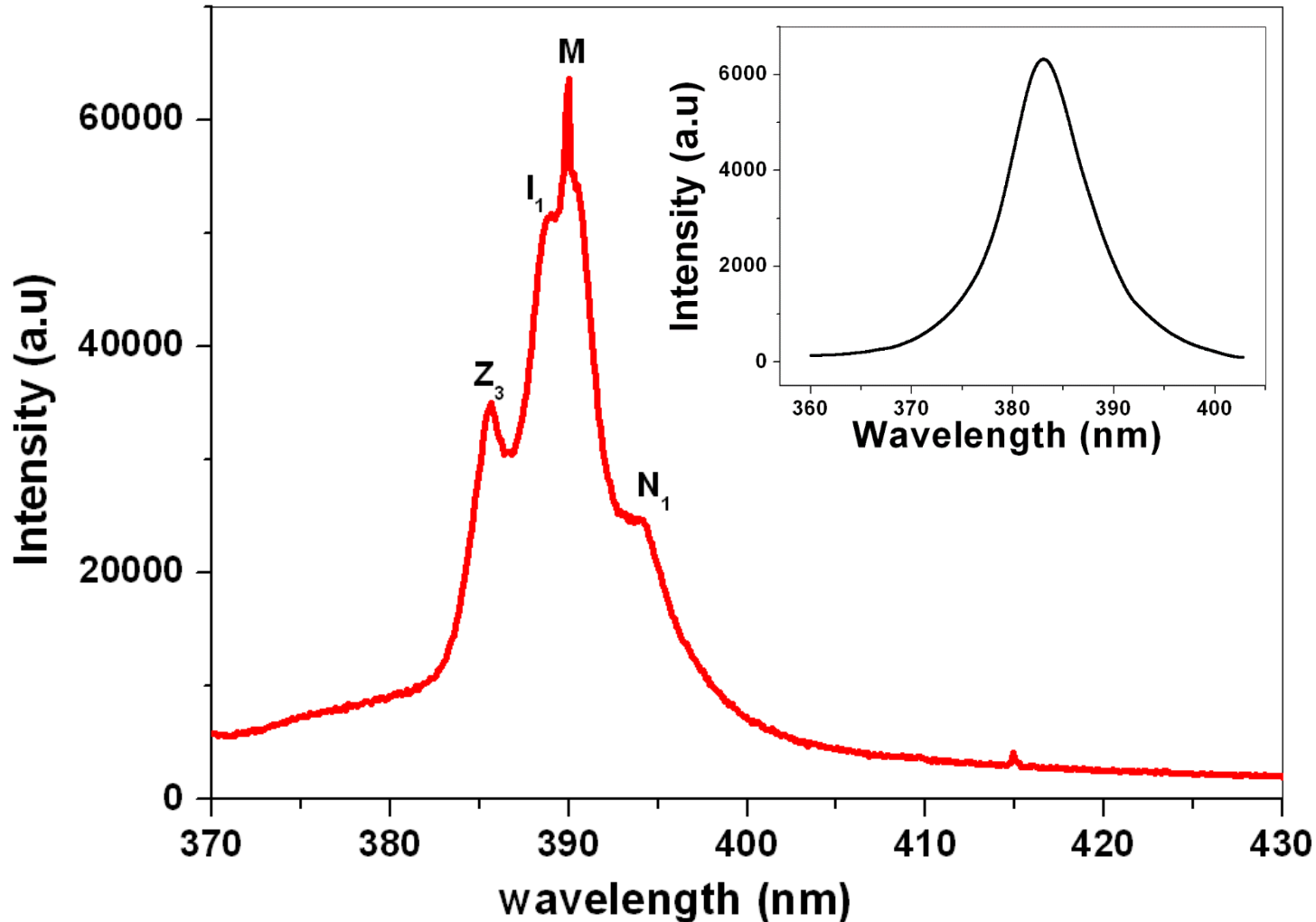
Source: K.V. Rajani *et al.*, *J. Phys. Condens. Matter* **25** (2013) 285501; K.V. Rajani *et al.*, *Thin Solid Films* **519** (2011) 6064; L. O'Reilly *et al.*, *J. Cryst. Growth* **287** (2006) 139.

XRD spectra of CuCl: Zn films



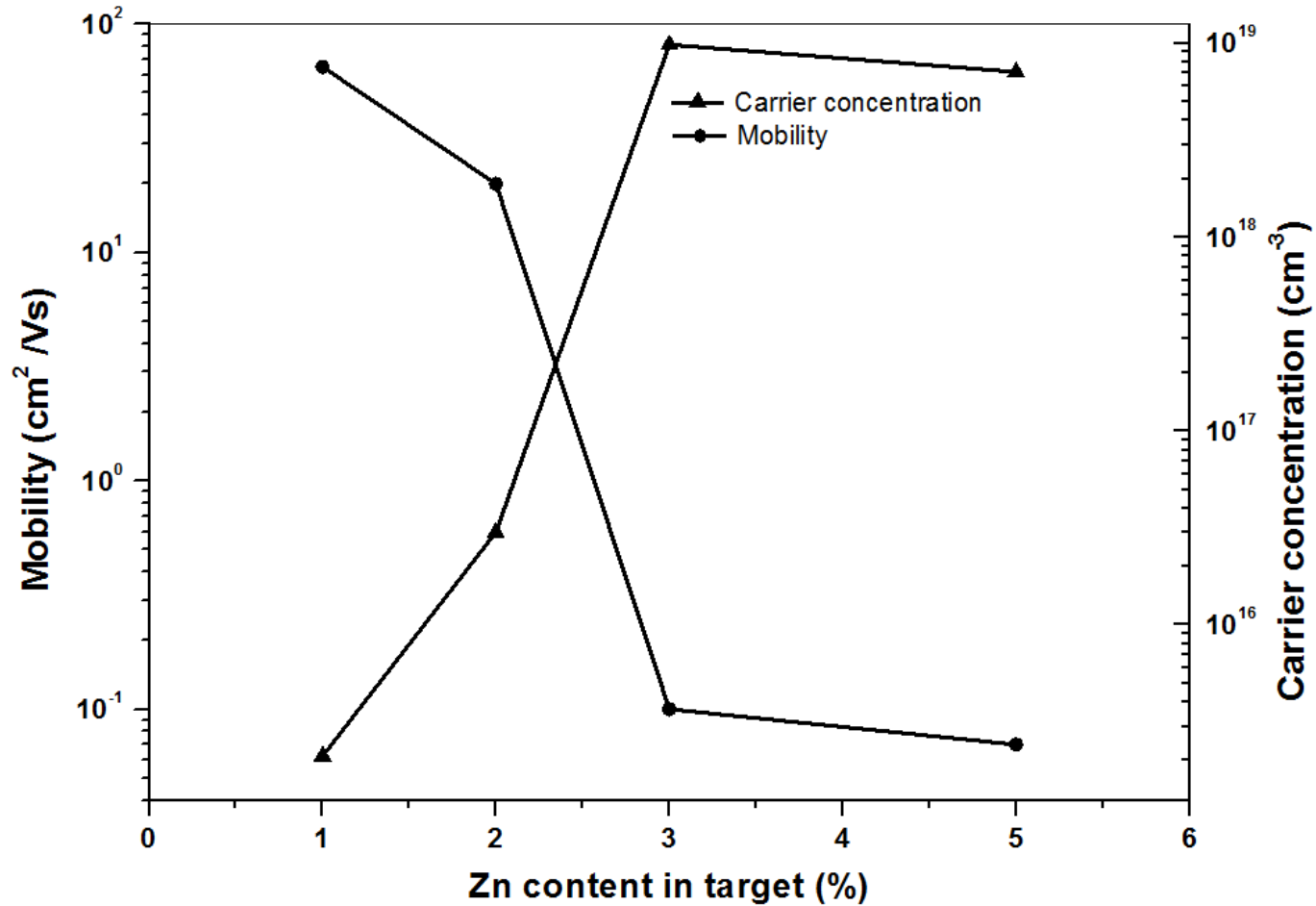
XRD of CuCl:Zn films developed from (a) 0, (b) 1, (c) 5 and (d) 3 wt % Zn doped targets and the intensity variation of (111) orientations (Inset)

Low temperature PL spectrum



PL spectrum at 80 K and at room temperature (inset) of a typical sample developed from 3wt % Zn doped target

Electrical properties



For 3% (w/w/) Zn

Carrier concentration $\approx 9.8 \times 10^{18} \text{ cm}^{-3}$
Carrier mobility $\approx 0.1 \text{ cm}^2\text{V}^{-1}\text{S}^{-1}$
Resistivity $\approx 6 \text{ }\Omega\text{cm}$

p-type CuHa nanolayers: O doping

p-CuBr (oxygen doped CuBr)

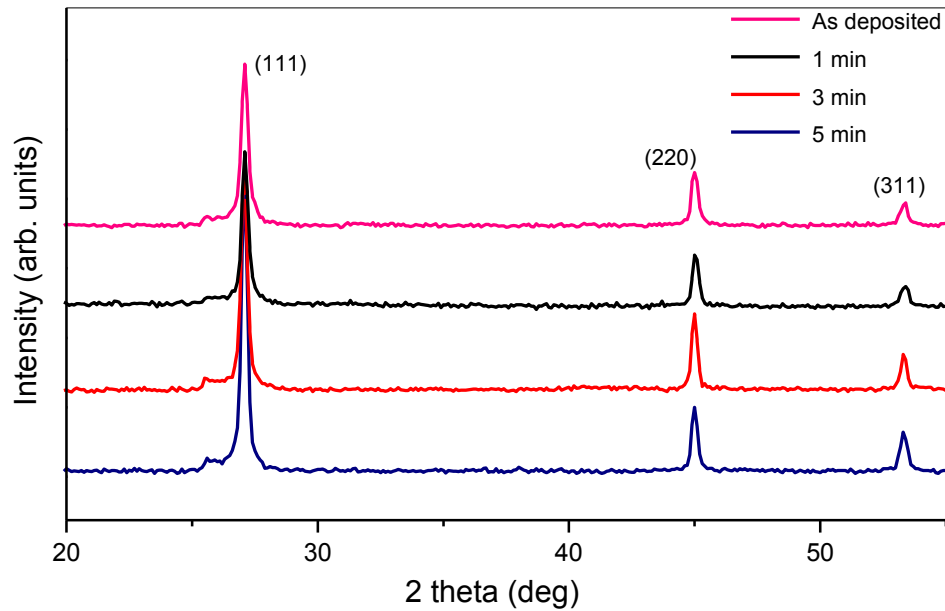


Physical Vapour Deposition (PVD) of CuBr powder followed by oxygen plasma treatment of the film

- Deposition pressure $\approx 3 \times 10^{-5}$ mbar
- Power ≈ 300 W
- Plasma chamber pressure $\approx 6.6 \times 10^{-2}$ mbar

Source: R.K. Vijayaraghavan *et al.*, *J. Phys. Chem. C* **118** (2014) 23226; K.V. Rajani *et al.*, *Mater. Letts.* **111** (2013) 63; D. Danieluk *et al.*, *J. Mater. Sci. Mater. Electron.* **20** (2009) 76.

p-type CuBr: Structure and Transparency

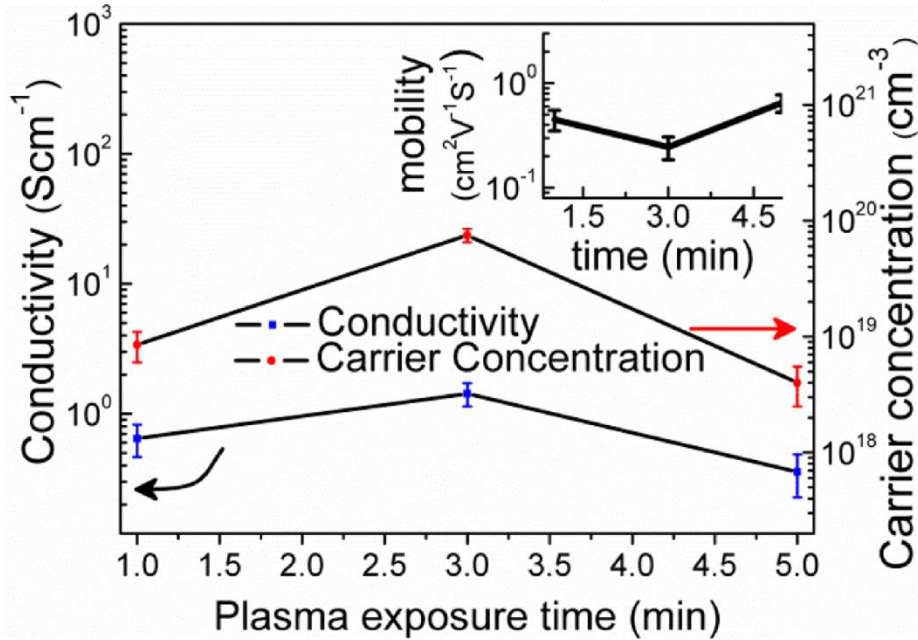


XRD pattern of the CuBr:O films

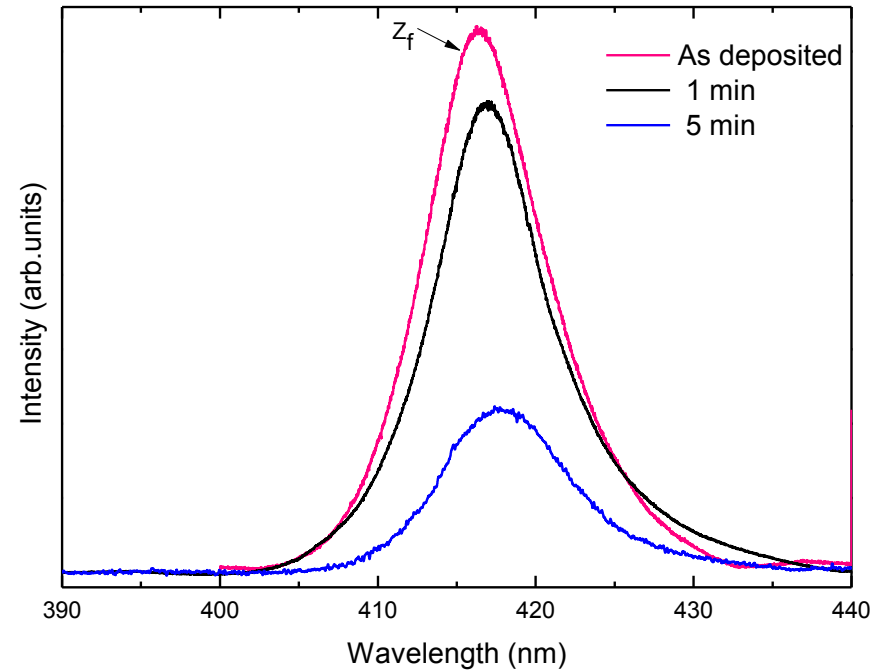


Photograph of the p-type CuBr film

Electrical & Optical Properties



Hole concentration and mobility



PL spectra of the of the ASD and oxygen doped CuBr film

1 min plasma exposure



Carrier concentration $\approx 8 \times 10^{18} \text{ cm}^{-3}$
Carrier mobility $\approx 0.5 \text{ cm}^2 \text{ V}^{-1} \text{ S}^{-1}$
Resistivity $\approx 1.5 \text{ } \Omega \text{ cm}$

Electrical contacts to CuHa layers

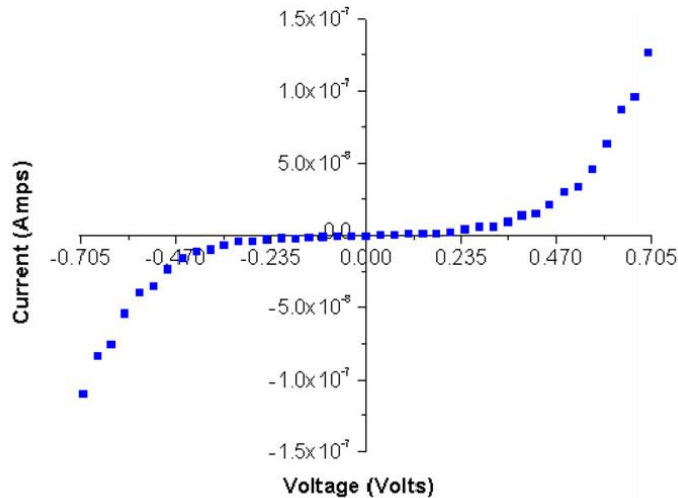


Figure 5. A typical room temperature I - V plot for a Au/CuCl/Au structure.

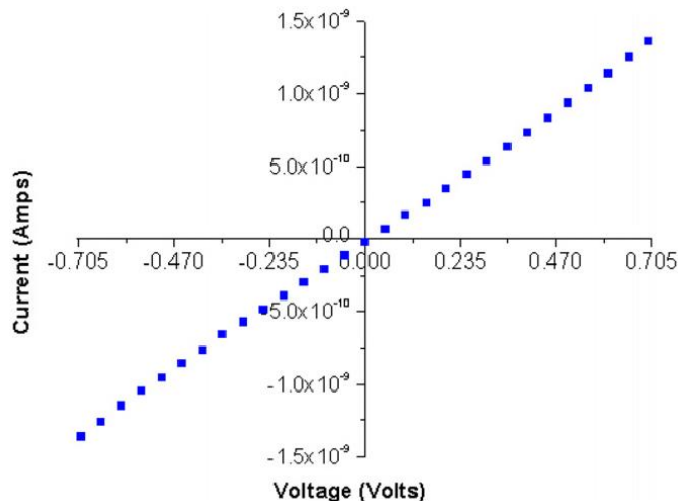
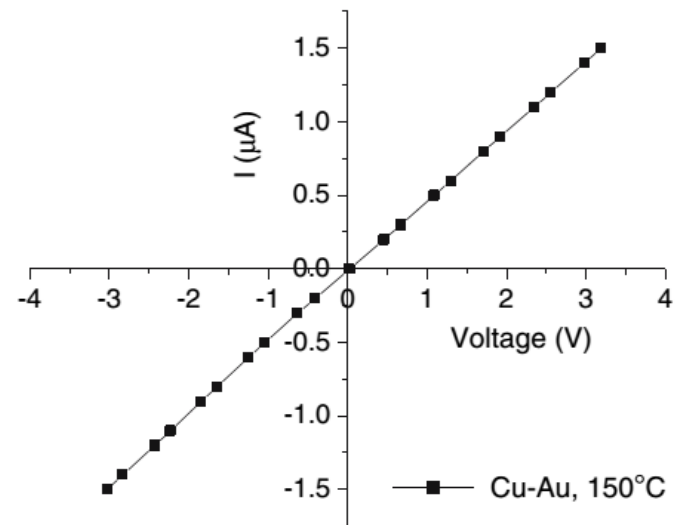


Figure 6. A typical room temperature I - V plot for a Cu/CuCl/Cu structure.

- Reversible Cu contacts: Cu^+ ions can be rapidly replaced with Cu.
- Irreversible Au: Cannot replenish Cu^+ ions \Rightarrow blocking electrode, non-Ohmic behaviour.

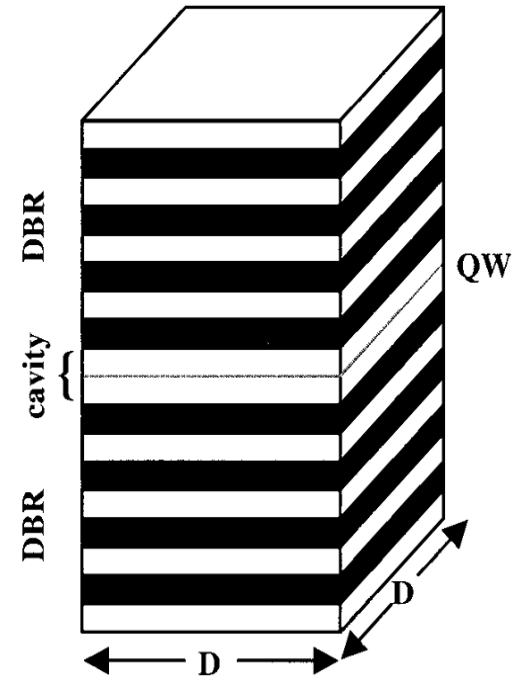


Co-evaporated Cu-Au contact to n-CuCl
($n \approx 10^{16} \text{ cm}^{-3}$)

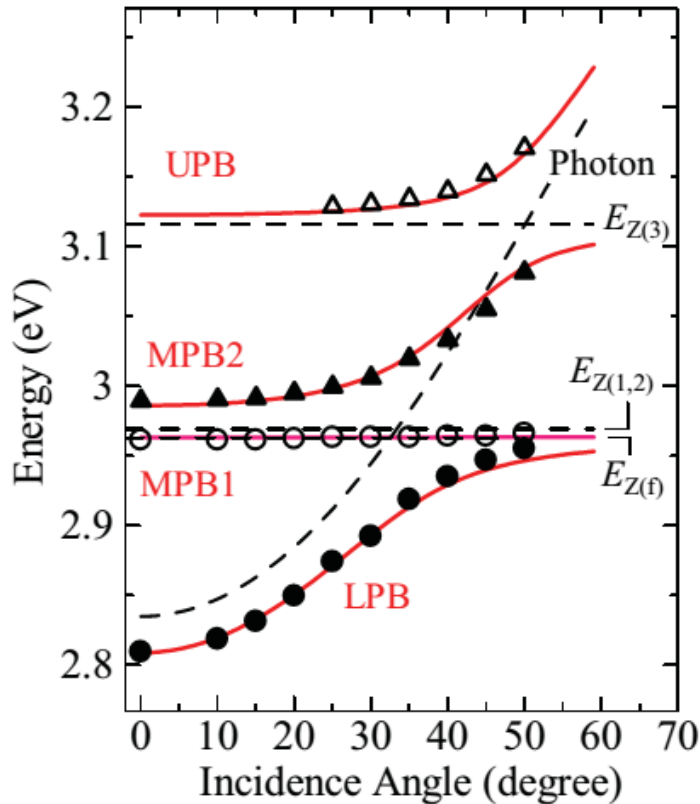
Source: F.O. Lucas *et al.* *J. Phys. D: Appl. Phys.* **40** (2007) 3461;
L. O'Reilly *et al.*, *J Mater Sci: Mater Electron.* **18** (2007) 57₂₅

Microcavity confinement for polaritons

- Distributed Bragg Reflectors (DBRs) are used:
- $\text{HfO}_2/\text{SiO}_2$ alternating layers (each layer tens of nm thick)
- Growth is typically on Al_2O_3 (0001) substrate.
- The effective active layer length is tied to the resonant wavelength of the CuHa excitons *in vacuo* and the background dielectric constant.
- Typical CuHa layer thicknesses of the order of 100 nm.
- DBRs and the CuHa: Physical vapour deposition.
- Angular dependence of reflectance spectra on incident light is used to prove the cavity polariton dispersion.
- Angle-resolved PL spectra are also used to confirm same.



CuBr Microcavity Polaritons



PL Spectra at 10 K

- CuBr active layer (thickness = $\lambda/2$) was sandwiched by the DBRs.
- $\lambda = \lambda_{EX}/\sqrt{\epsilon_b}$ in a bulk microcavity; λ_{EX} is the resonant wavelength of the lowest lying exciton in vacuum, and ϵ_b is the background dielectric constant.
- $\lambda/2 = 88$ nm, and $\epsilon_b = 5.7$.
- DBRs = HfO₂/SiO₂ (9.5 periods (top) and 8.5 periods (bottom))
- **Four cavity-polariton modes:** Lower Polariton Branch (LPB), Middle Polariton Branch 1 (MPB1), Middle Polariton Branch 2 (MPB2), and Upper Polariton Branch (UPB) in order of energy
- Incidence-angle PL dependence of the energies of the four cavity-polariton modes.
- Solid curves depict the fitted results with theory.
- Dashed horizontal lines indicate the exciton energies, and the dashed curve shows the cavity-photon dispersion.

Advantages of CuHa for Polariton Lasing

Number of active region Quantum Wells (QWs)

	GaAs	CdTe	CuCl
Bohr Radius in QW (Å)	90	28	7
Binding Energy(meV)	10	25	190
Saturation Density of Lower Polaritons (10^{10} cm^{-2})	4	50	20,000

Adopted from:

H. Deng *et al.*, Rev. Mod. Phys. **82** (2010) 1489-1537.

➔ Use of multiple QWs – enhances E-field/exciton overlap

$$\Omega_{\text{Rabi}} \propto \sqrt{N_{\text{QW}}}$$

$$n_{\text{exc}} \propto 1/N_{\text{QW}} \quad \text{for a given polariton population}$$

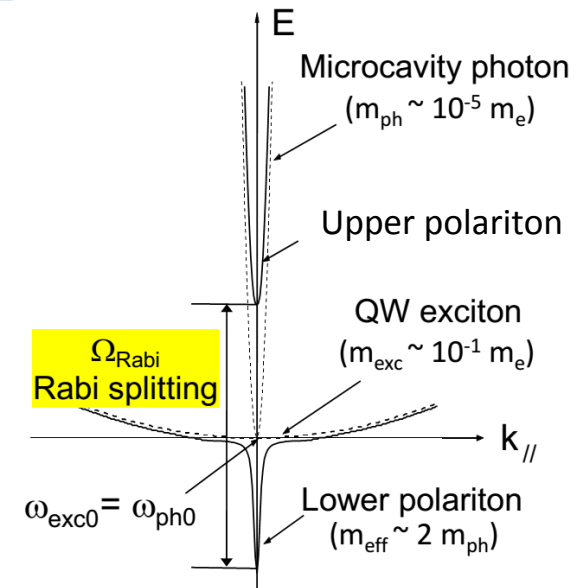
↓
12 GaAs MQWs

➔ Use of excitons with small Bohr radius

$$n_{\text{sat}} \propto 1/a_B^{*2}$$

↓
CdTe DQW

➔ **1 QW (pn junction) for CuHa?**



Multiple Deposition Possibilities

- Thin (<100 nm) CuHa nanolayers can be deposited using:
 - Physical Vapour Deposition (RF / Pulsed DC magnetron sputtering)
 - Electron beam deposition
 - Atomic layer deposition
- All produce CuHa materials of sufficient quality to confirm polaritonic modes and the presence of biexcitons.

JOURNAL OF APPLIED PHYSICS **112**, 033505 (2012)

Study of exciton-polariton modes in nanocrystalline thin films of CuCl using reflectance spectroscopy

Barry Foy,^{1,a)} Enda McGlynn,^{1,b)} Aidan Cowley,² Patrick J. McNally,² and Martin O. Henry¹

¹*School of Physical Sciences, National Centre for Plasma Science and Technology, Dublin City University, Glasnevin, Dublin 9, Ireland*

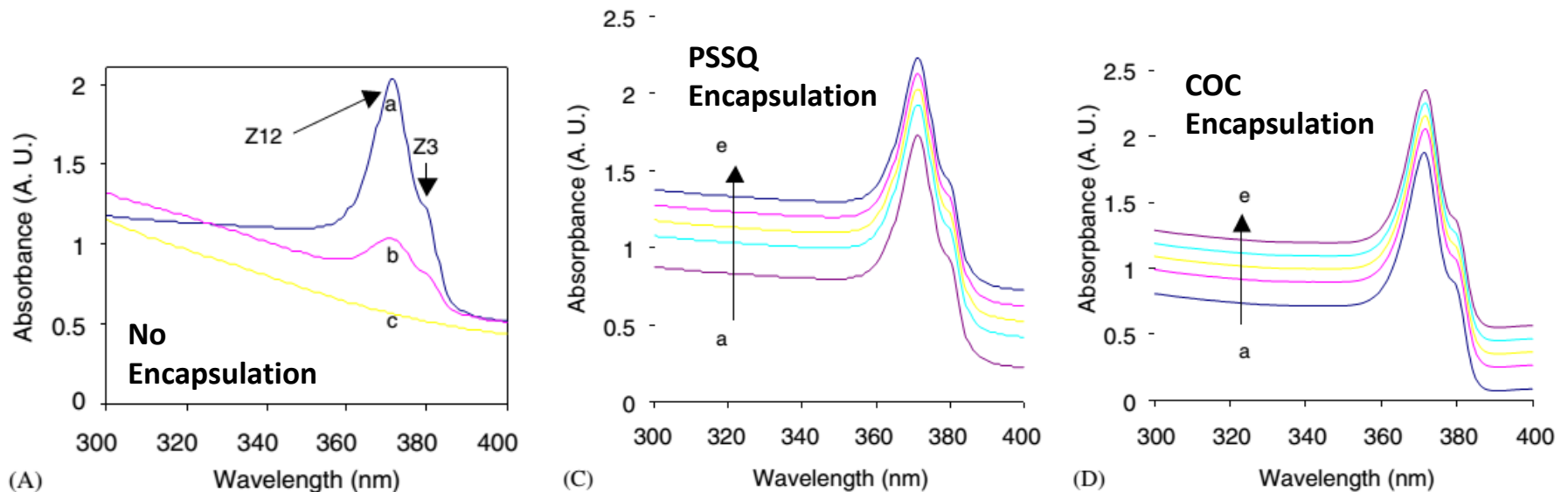
²*Nanomaterials Processing Laboratory, The Rince Institute, School of Electronic Engineering, Dublin City University, Dublin 9, Ireland*

(Received 2 May 2012; accepted 27 June 2012; published online 2 August 2012)

CuCl thin films grown on (100) Si by thermal evaporation are studied using reflectance spectroscopy. The reflectance spectra in the near UV spectral range close to the CuCl bandgap are modeled using a dielectric response function based on an exciton-polariton response with various models involving dead layers and reflected waves in the thin film. The exciton-polariton structure obtained is compared to other studies of bulk CuCl crystals. These different models are analyzed using a matrix-based approach and they yield theoretical spectra of reflected intensity. The fits provide parameter values which can be compared to bulk data known for CuCl and provide a non-destructive means of quantitative analysis of CuCl thin films. The best models are shown to match the experimental data quite well, with the closest fits produced when thin film front and rear interfaces are included. This model also accurately simulates the Fabry-Perot fringes present at energies lower than the Z_3 free exciton position in CuCl (at 3.272 eV). © 2012 American Institute of Physics. [<http://dx.doi.org/10.1063/1.4739726>]

Device Encapsulation

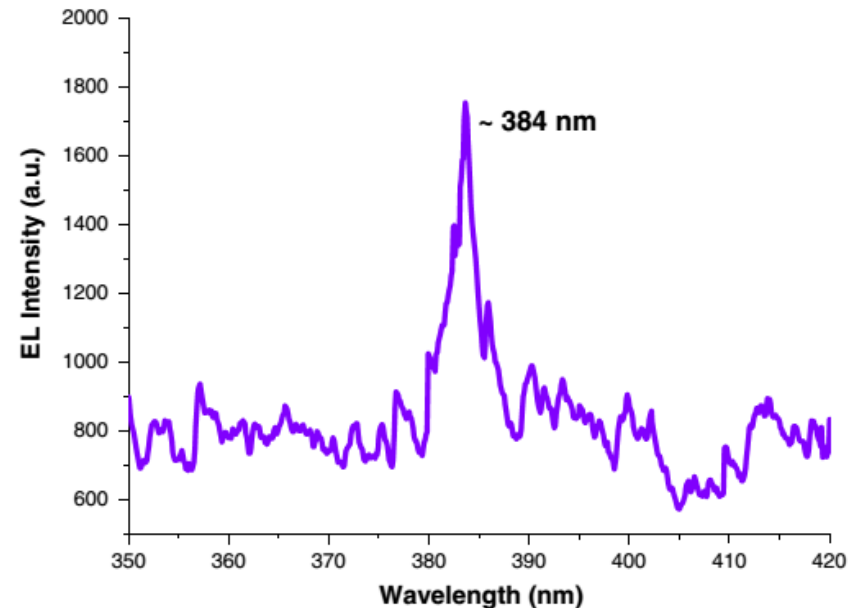
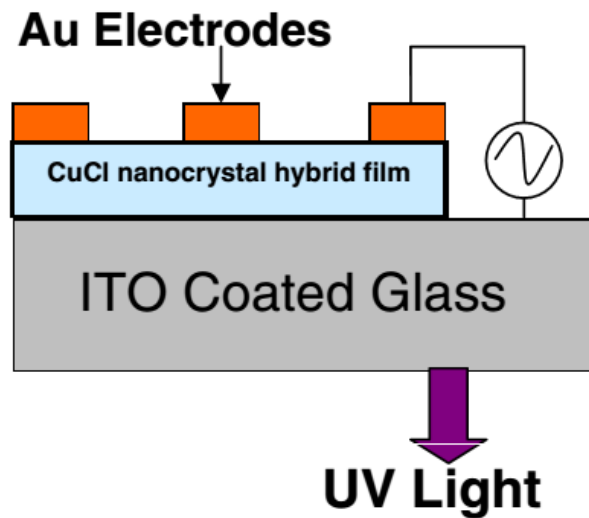
- Polysilsesquioxane-based spin on glass material (PSSQ).
- Cyclo olefin copolymer (COC) thermoplastic-based materials.
- CuCl optical properties unaltered for up to 28 days.



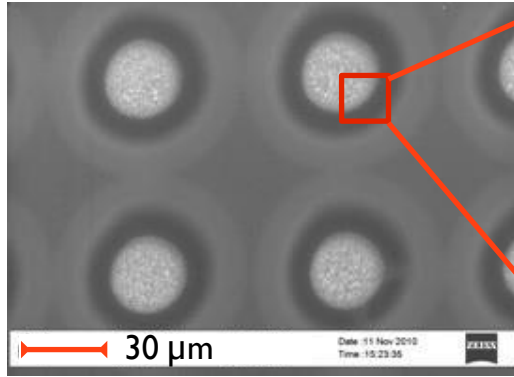
Absorbance spectra: (a) immediately after deposition, (b) 7 days, (c) 14 days, (d) 21 days, (e) 28 days. [Plots shifted with respect to each other for ease of visibility.]

Other Growth Options

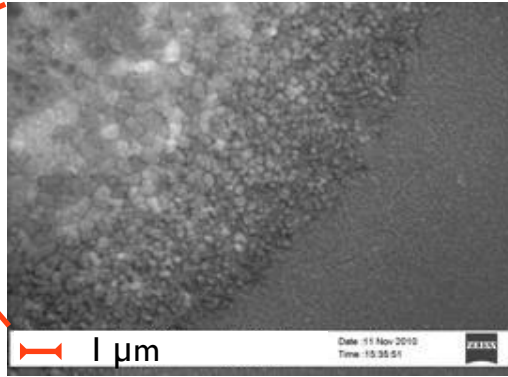
- Hybrid organic-inorganic spin-on-glass CuCl films
– PSSQ/CuCl.



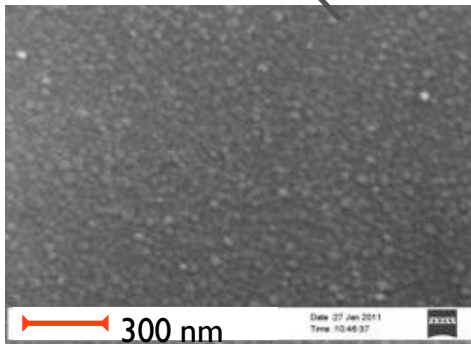
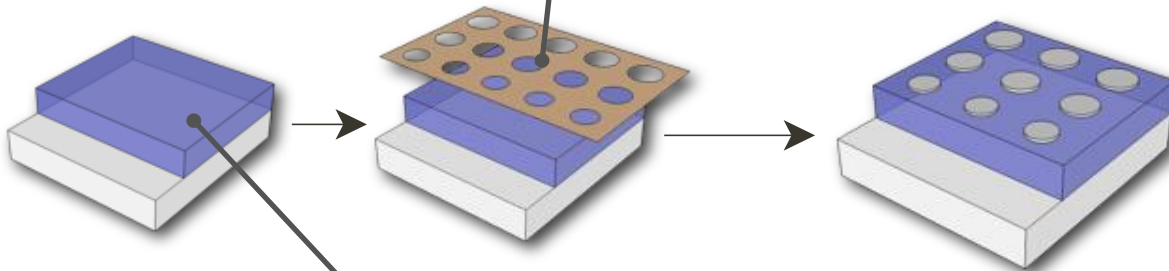
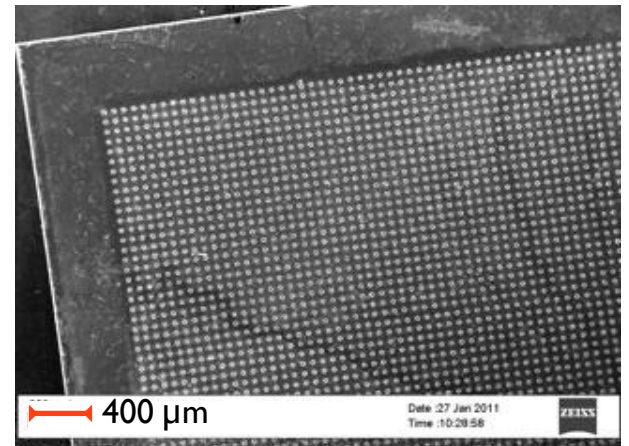
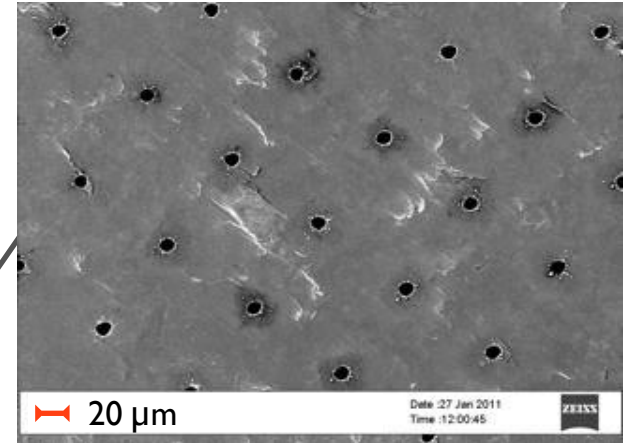
Vapour Liquid Solid (VLS) Growth of CuBr/KBr Microdots



KBr 'Spots'



Shadow Mask

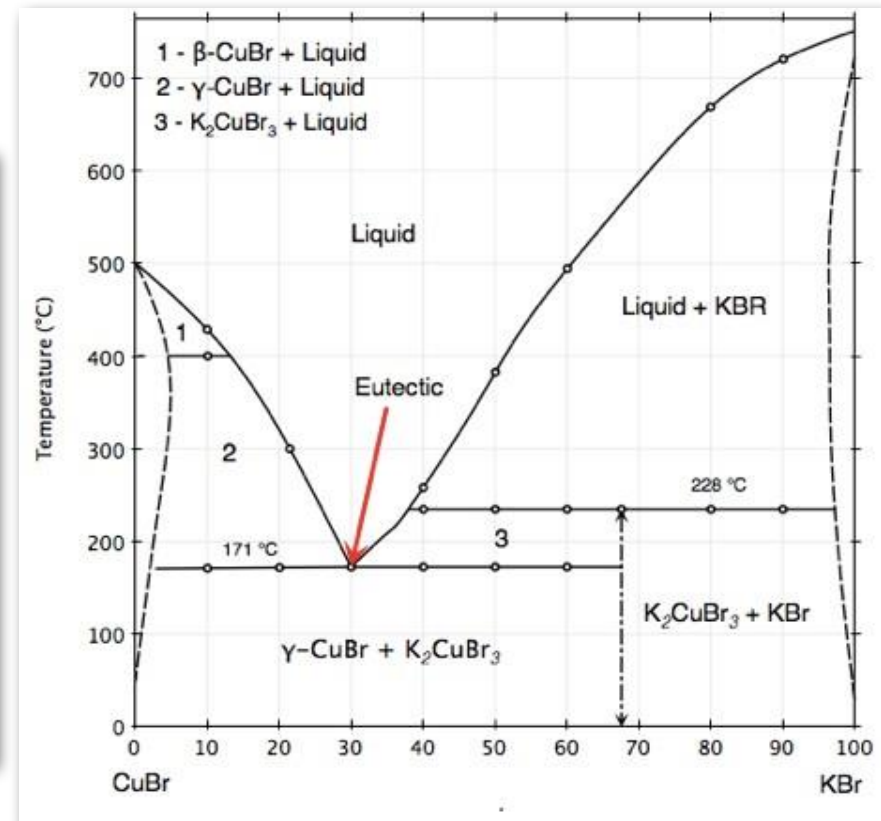
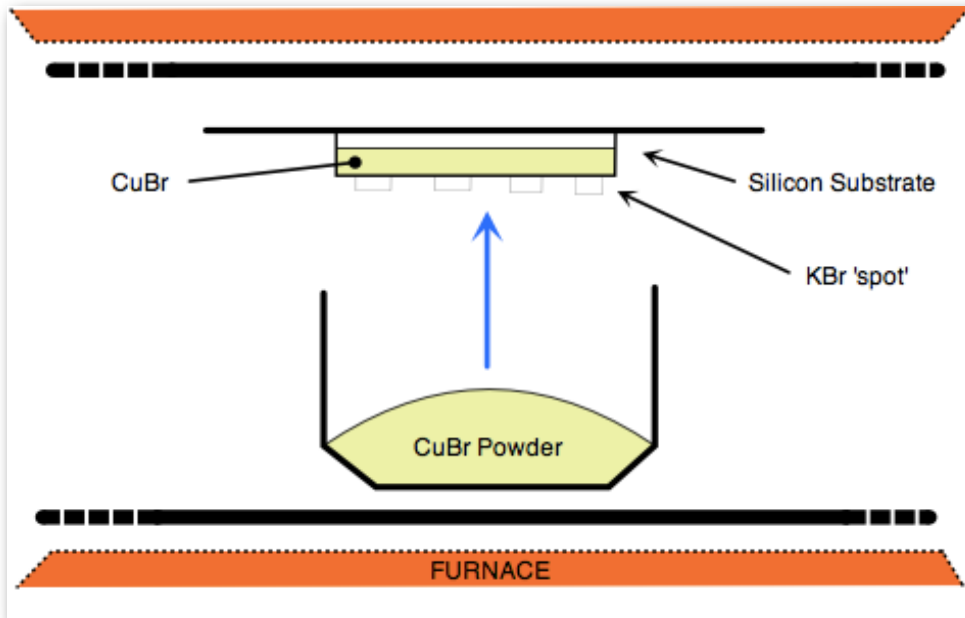


Evaporated CuBr

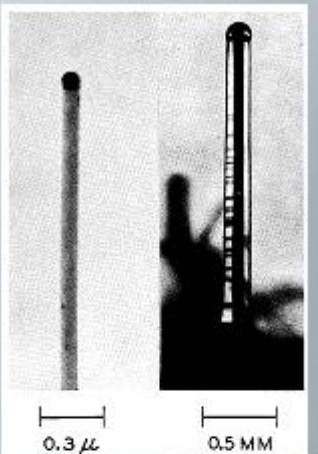
~350nm CuBr evaporated film on Si

Intermixed CuBr/KBr Microdot VLS Formation

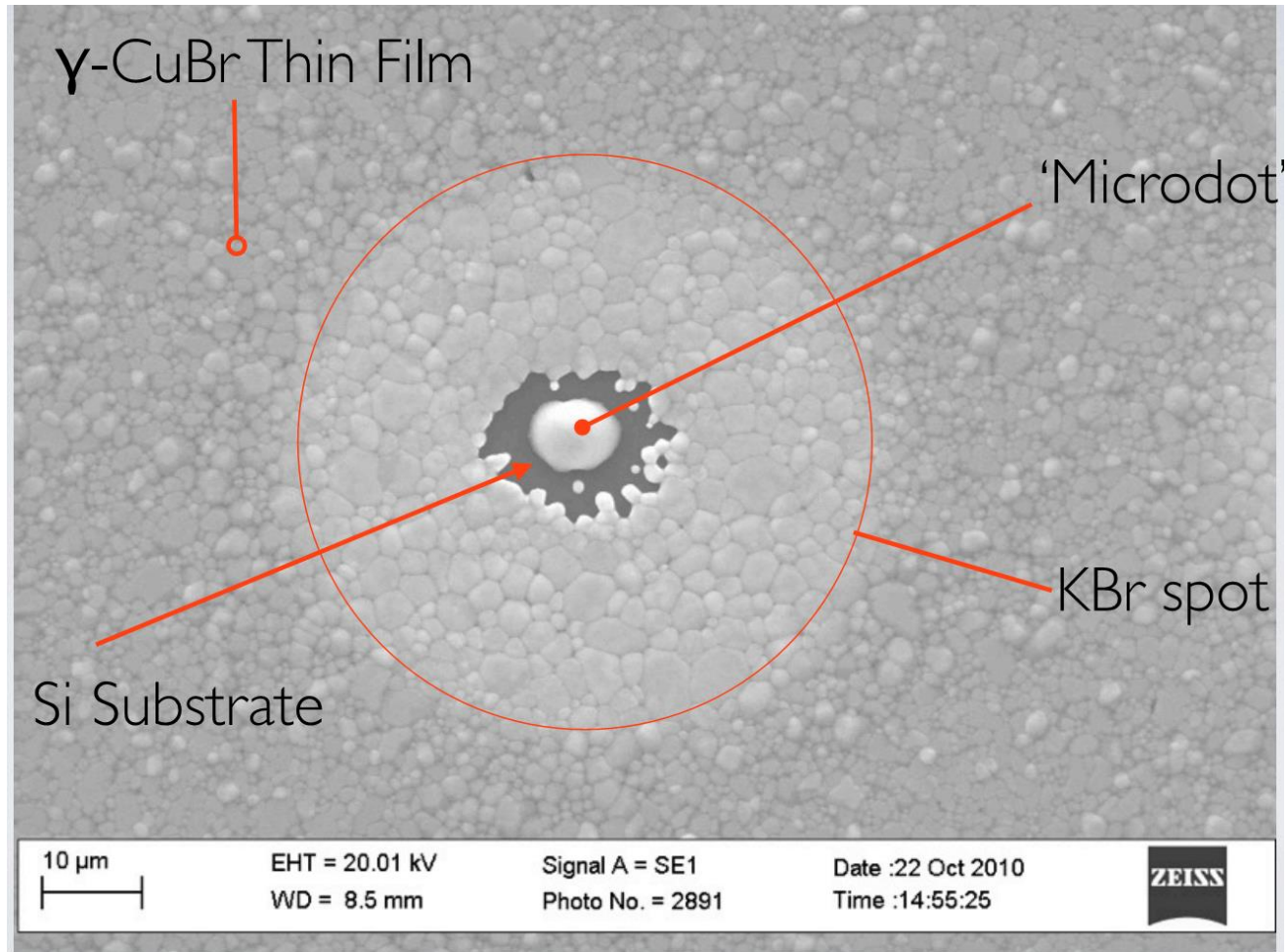
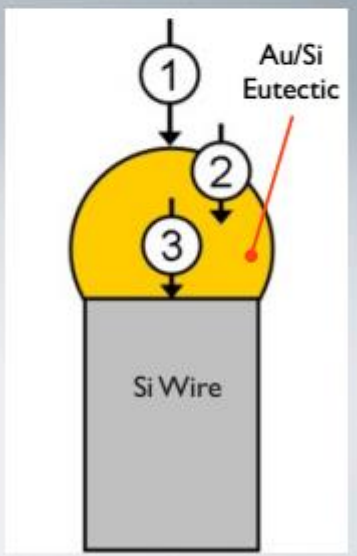
- After shadow mask deposition of KBr, films are annealed at 220° C under vacuum.
- In addition, a small flux of CuBr is provided.
- The CuBr/KBr phase diagram shows that a eutectic solution will form at approximately 170°C.



CuBr/KBr Intermixed Microdot

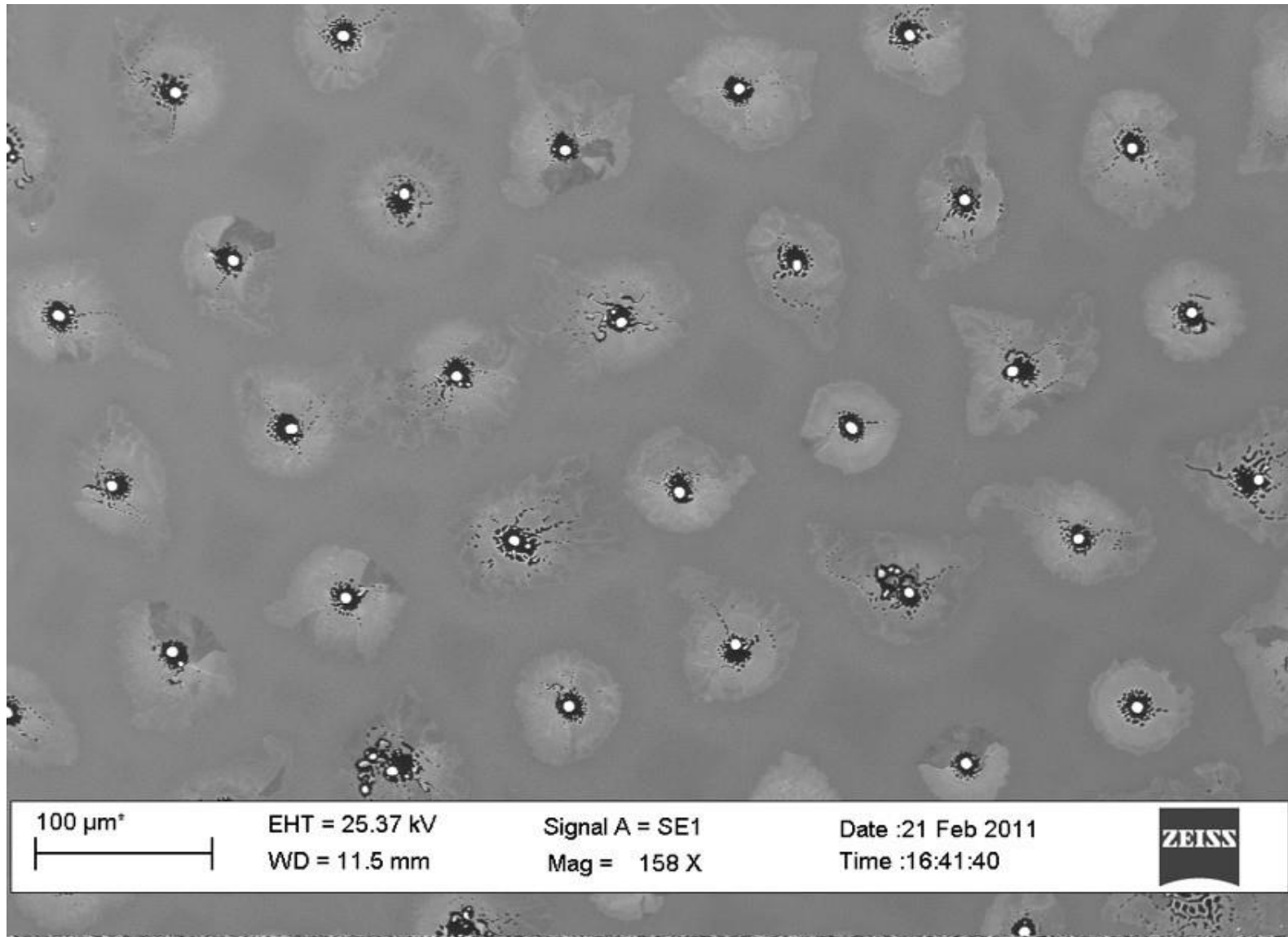


R. Wagner and W. Ellis, "VAPOR-LIQUID-SOLID MECHANISM OF SINGLE CRYSTAL GROWTH," Applied Physics Letters, 1964.



- Inspiration: Silicon 'whiskers' grown using VLS type growth since the early 1960's.
- Nanowires /nanorods ⇒ single crystals with fewer imperfections.

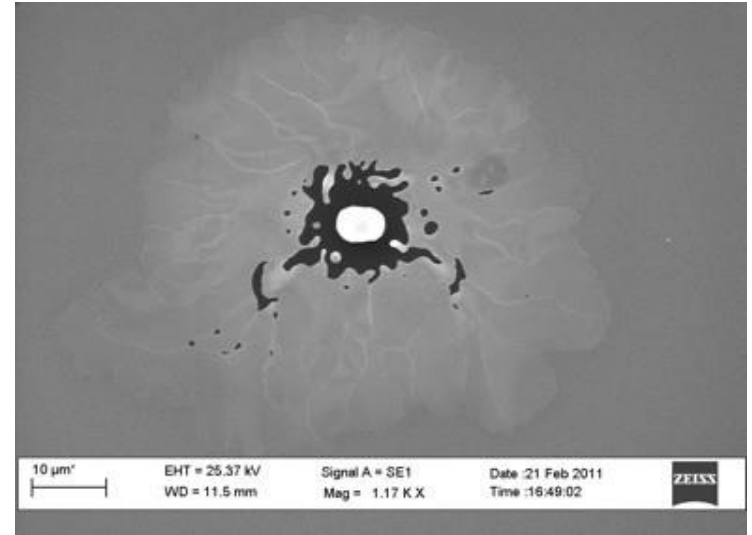
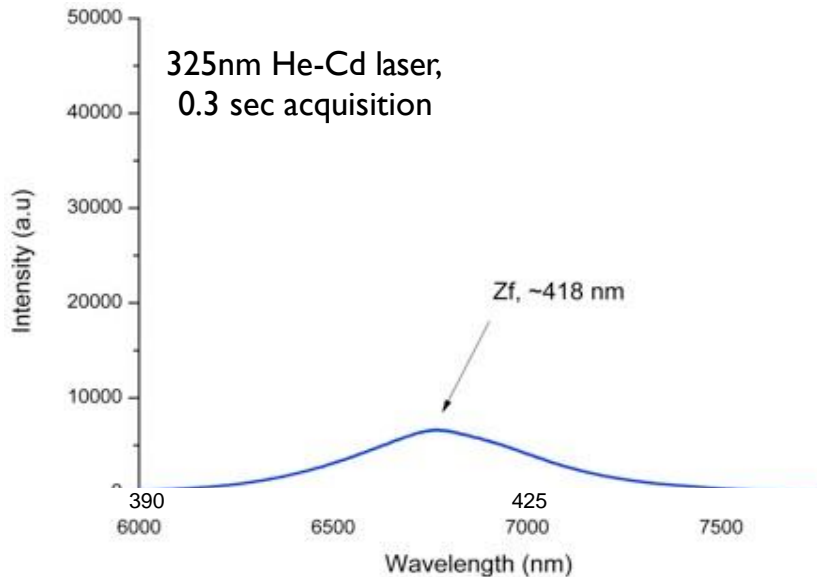
CuBr/KBr Microdot Array



Room Temperature PL

Room Temperature PL Enhancement

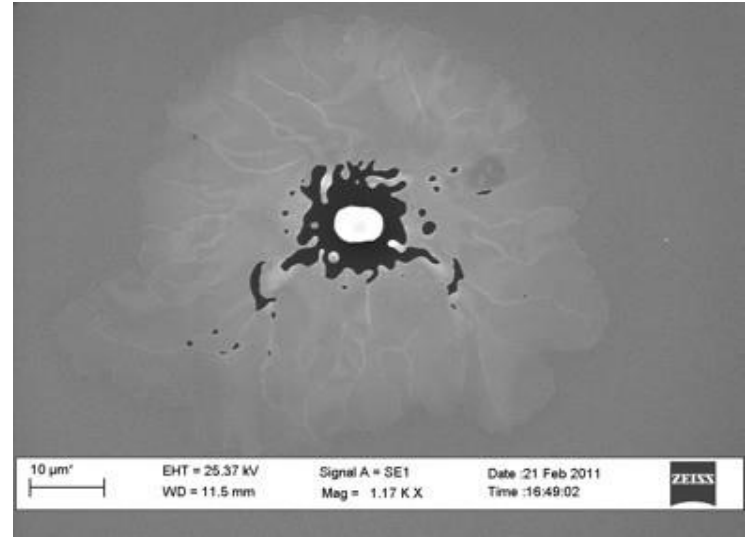
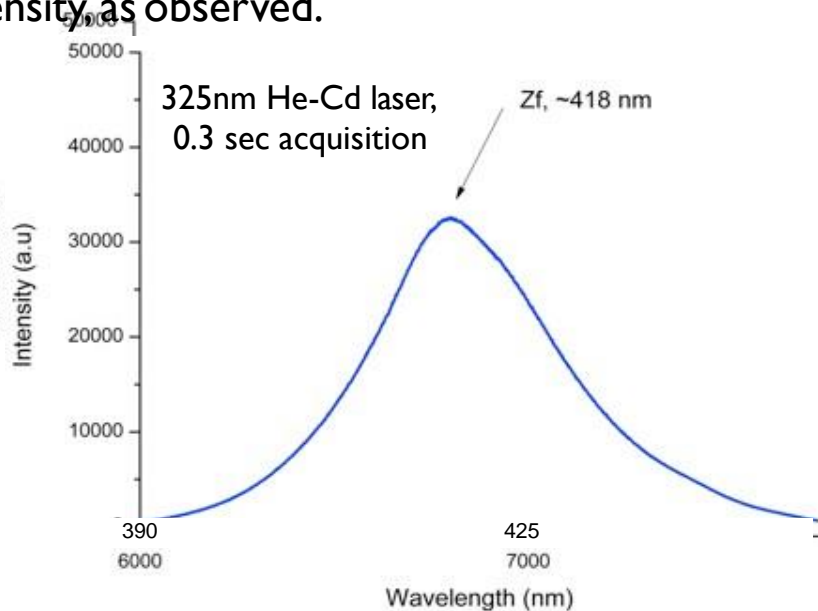
- Observed luminescence improvement is based on the migration of Cu^+ and K^+ ions within the film.
- Crystalline imperfections can act as recombination centres, trapping electrons and holes and reducing the effective carrier concentration for emission processes.
- Displacement of the Cu^+ and K^+ ions, driven by their chemical affinities for negative ions (i.e., the Br^- anion), can close some of the vacancies present [1].
- Can result in a net improvement of the emission intensity, as observed.



Room Temperature PL

Room Temperature PL Enhancement

- Observed luminescence improvement is based on the migration of Cu^+ and K^+ ions within the film
- Crystalline imperfections can act as recombination centers, trapping electrons and holes and reducing the effective carrier concentration for emission processes.
- Displacement of the Cu^+ and K^+ ions, driven by their chemical affinities for negative ions (i.e., the Br^- anion), can close some of the vacancies present [1].
- Can result in a net improvement of the emission intensity as observed.



Where next?

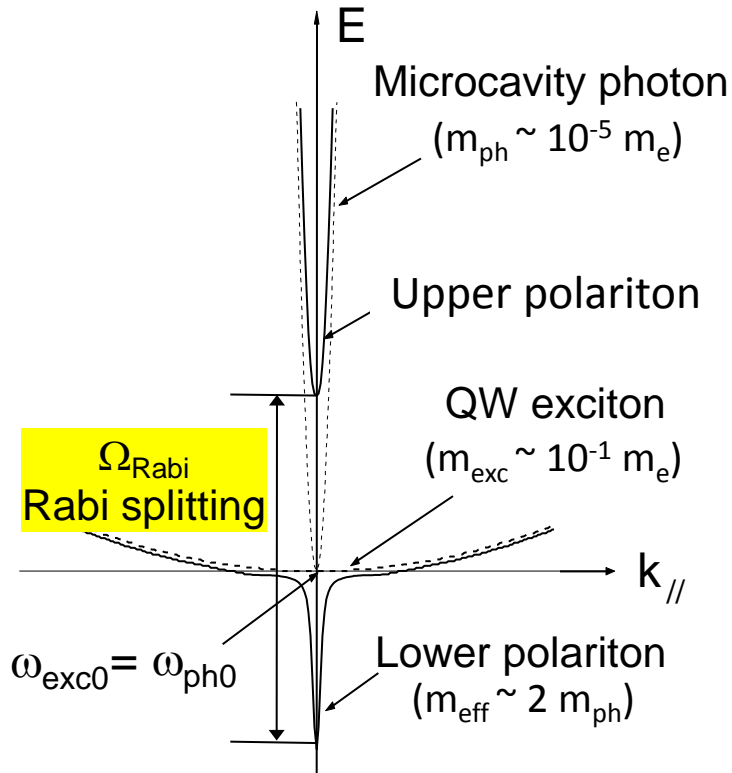
- Excellent progress in CuHa materials processing in past decade.
- Opportunity to develop new science, technology and devices.
- Quantum manipulation of light and matter for blue/UV (350-450 nm).
- Electrically pumped microcavity structures.
- Ultralow power blue/UV light emitters.
 - Exciton, biexciton and polariton control.
 - Potential for quantum entanglement.
- **Applications:**
 - Medical and biodiagnostics: new capability in point of care diagnostics;
 - Computing : extremely low power optical interconnects;
 - Telecommunications: THz speed optical spin switching;
 - Security/cryptography: quantum entanglement for quantum information processing communications;
 - Who knows???

THANK YOU!!!

Exciton Polariton Dispersion, Normal Mode Splitting and Oscillation

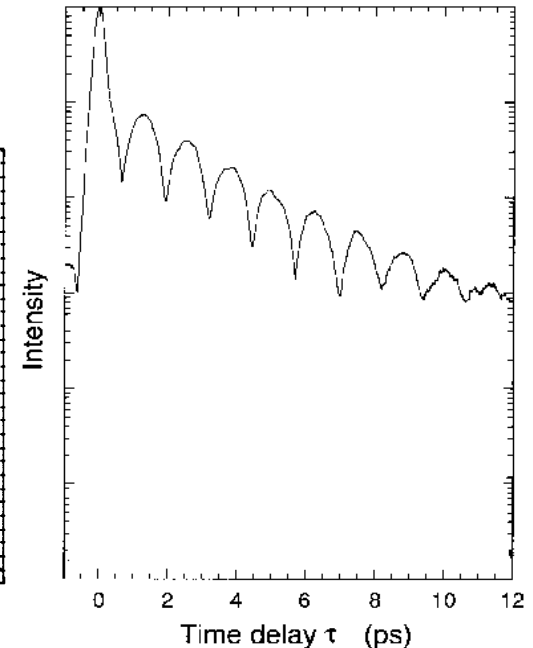
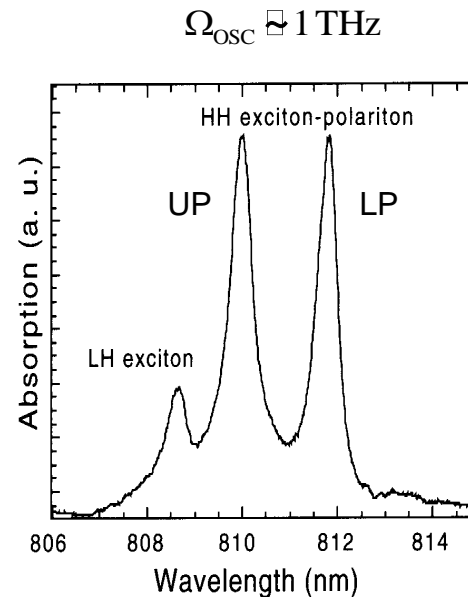
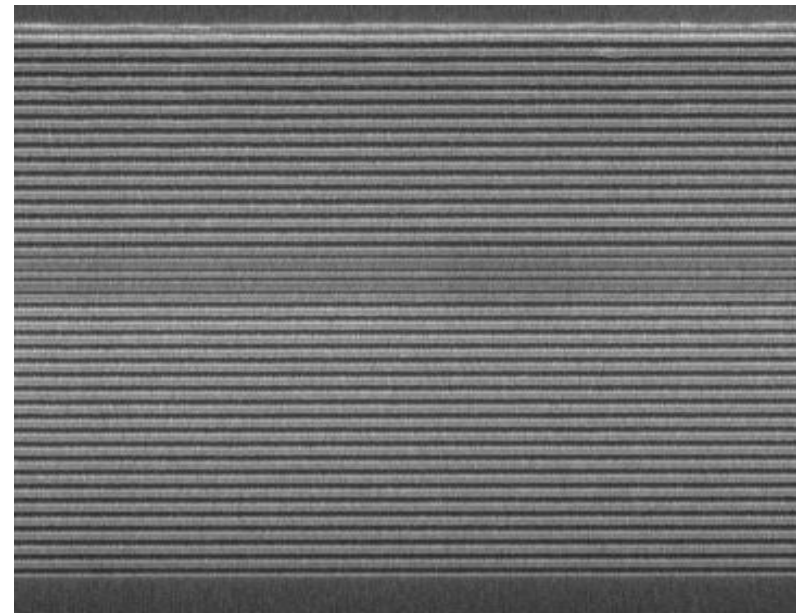
[H. Deng et al., BaCa Tec-Summer School, Würzburg, Germany
(2005)]

Polariton dispersion curves



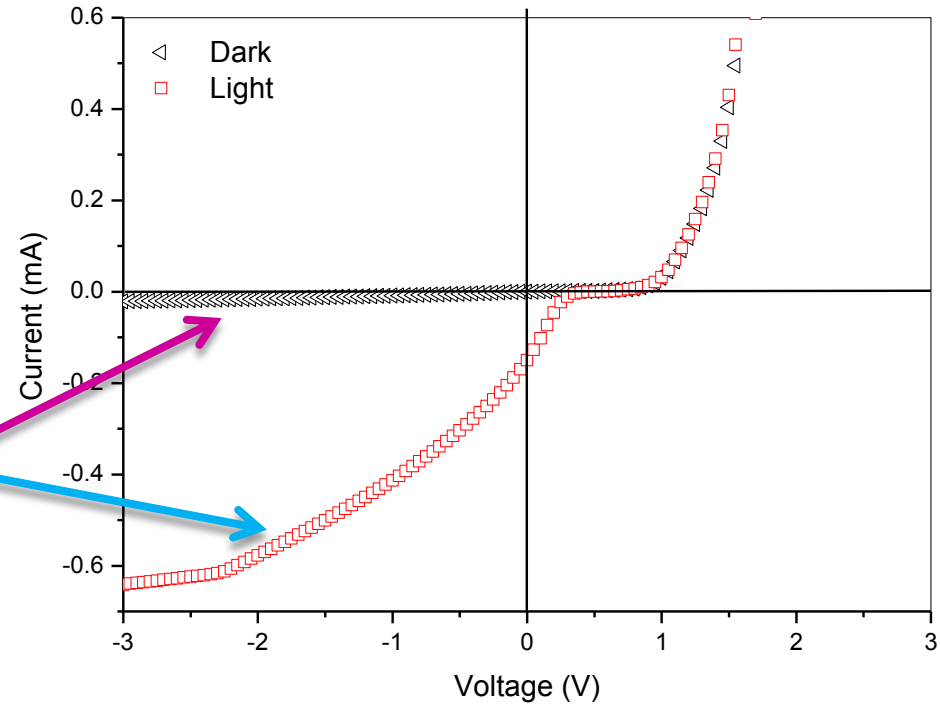
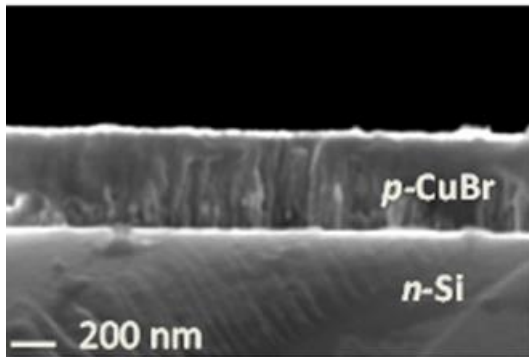
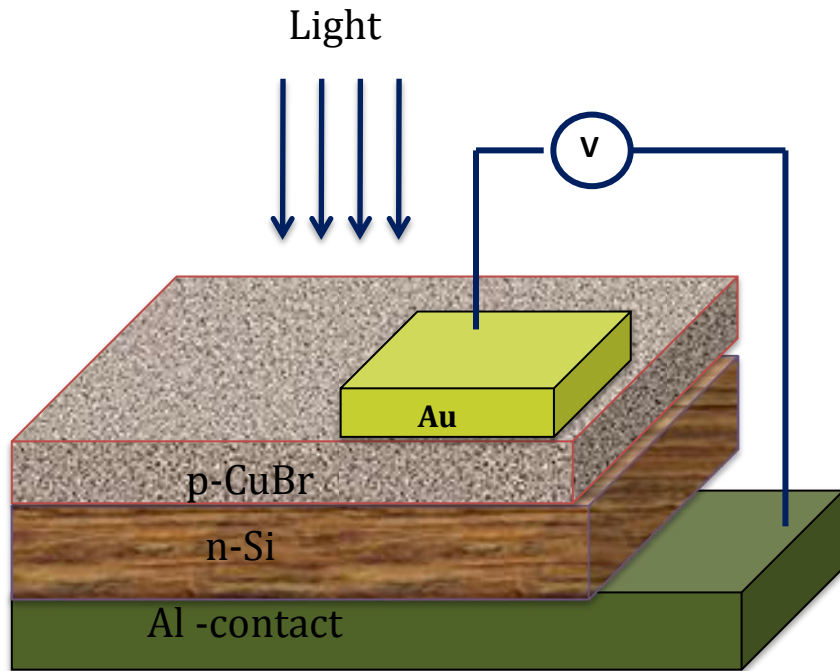
C. Weisbuch, *et al. Phys. Rev. Lett.* **69**
(1992) 3314.

GaAs/AlGaAs Systems



S. Jiang *et al., Appl. Phys. Lett.* **73** (1998) 3031.

CuBr/Si heterojunction for photovoltaic applications



I-V characteristics in dark and under illumination

Efficiency of $\approx 2.1\%$ with AM1.5 illumination

Polariton Device Structures

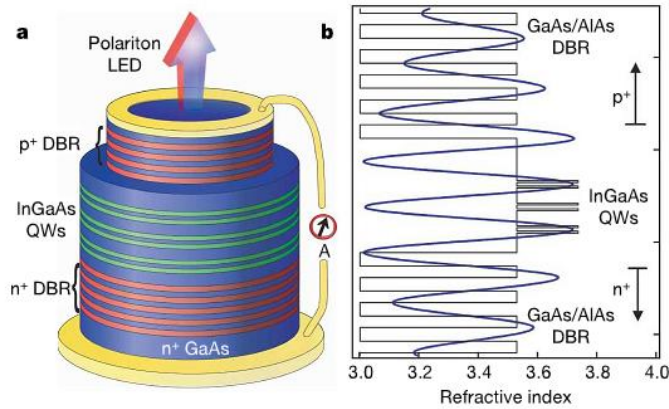


Figure 1 | Schematic sketch of the polariton microcavity LED. **a**, The structure consists of a $5\lambda/2$ cavity surrounded by two doped GaAs/AlAs DBRs. Dry etching was used to expose the p-DBR, forming round mesas of $400\ \mu\text{m}$ diameter. To enable light emission from the front side, a ring-shaped p-type ohmic contact was deposited on the top of the mesa, and the n-type contact was deposited on the back side of the substrate. QW, quantum well. Current source A is used to bias the device. **b**, Electric field and refractive index distribution along the structure. Elevated temperatures necessitate the use of three pairs of $\text{In}_{0.1}\text{Ga}_{0.9}\text{As}/\text{GaAs}$ quantum wells placed at the antinodes of the electric field to enhance the exciton oscillator strength required for strong coupling.

Nature **454** (2008) 372- S.I.
Tsintzos *et al.*

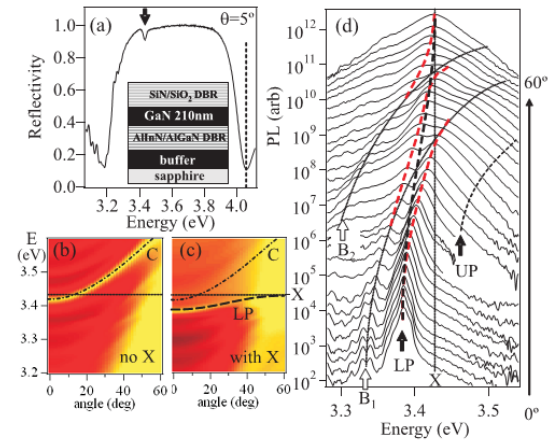


FIG. 1 (color online). (a) Microcavity reflectivity at 300 K and $\theta \sim 5^\circ$, with lower polariton mode marked (arrow). Dashed line shows nonresonant pump energy. Inset shows the layer structure. (b), (c) Theoretical angular dispersion both without (b) and with (c) the resonant exciton contribution to the GaN cavity (ω_{LP} dashed line, ω_{cav} dash-dotted line) for a slightly negatively detuned cavity ($\Delta = -10\ \text{meV}$). (d) Angle-resolved PL at low powers up to 60° , with lower (LP) and upper (UP) polaritons, exciton (X), and Bragg modes (B) marked.

PRL **98** (2007)126405 - S.
Christopoulos *et al.*

Polariton Device Structures

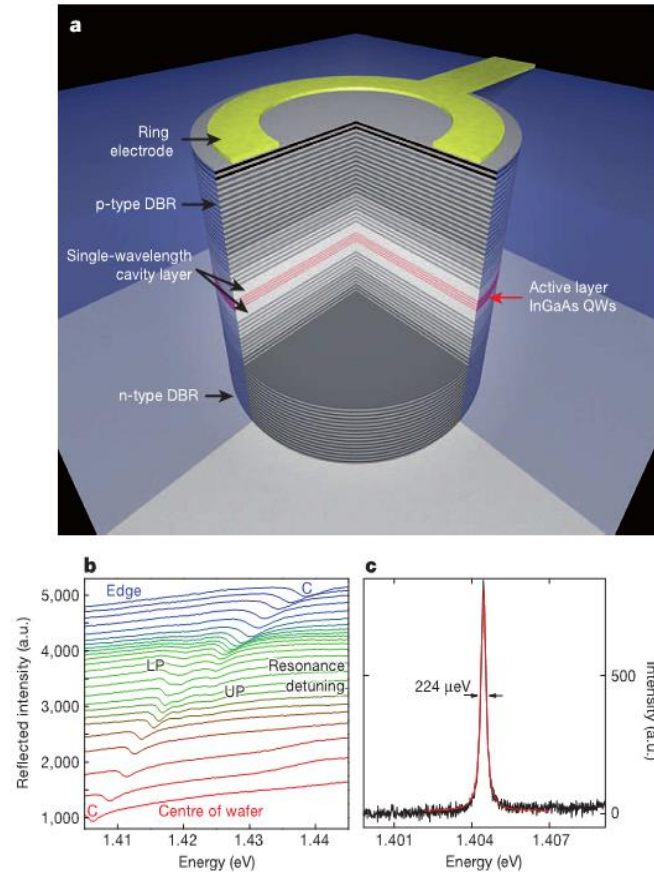


Figure 1 | Quantum well microcavity polariton diode and characteristics.
a, Schematics of an electrically contacted 20- μm -diameter micropillar with four quantum wells (QWs) in the cavity, sandwiched by gradually doped distributed Bragg reflectors (DBRs). **b**, Waterfall plot of reflectivity spectra showing anticrossing on the detuning map. a.u., arbitrary units; LP, lower polariton; UP, upper polariton; C, photonic cavity mode. **c**, Microphotoluminescence spectrum of the fundamental mode of a highly photonic micropillar cavity with a diameter of 2 μm and $Q \approx 6,320$.